POR-2210(EX)
WT-2210(EX)
EXTRACTED VERSION

OPERATION SUN BEAM, SHOT SMALL BOY

Project Officer's Report—Project 2.2

Measurement of Fast-Neutron Dose Rate as a Function of Time

S. Kronenberg, Project Officer
B. Markow
I. A. Balton
U. S. Army Electronics Research and Development Laboratory
Fort Monmouth, NJ

11 October 1963

NOTICE:

This is an extract of POR-2210 (WT-2210), Operation SUN BEAM, Shot Small Boy, Project 2.2.

Approved for public release;
distribution is unlimited.

Extracted version prepared for
Director
DEFENSE NUCLEAR AGENCY
Washington, DC 20305-1000

1 September 1985

DISCLAIMER NOTICE

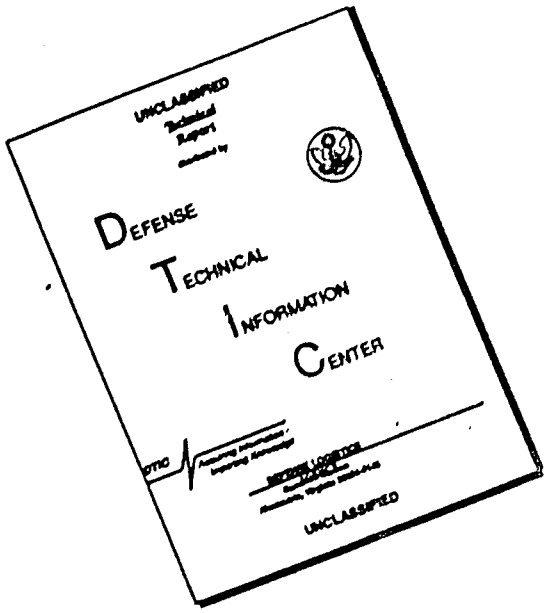

THIS DOCUMENT IS BEST QUALITY AVAILABLE. THE COPY FURNISHED TO DTIC CONTAINED A SIGNIFICANT NUMBER OF PAGES WHICH DO NOT REPRODUCE LEGIBLY.

Destroy this report when it is no longer needed. Do not return to sender.

PLEASE NOTIFY THE DEFENSE NUCLEAR AGENCY, ATTN: STTI, WASHINGTON, DC 20305-1000, IF YOUR ADDRESS IS INCORRECT, IF YOU WISH IT DELETED FROM THE DISTRIBUTION LIST, OR IF THE ADDRESSEE IS NO LONGER EMPLOYED BY YOUR ORGANIZATION.

UNCLASSIFIED
SECURITY CLASSIFICATION OF THIS PAGE

AD-A995 372

REPORT DOCUMENTATION PAGE

1a REPORT SECURITY CLASSIFICATION UNCLASSIFIED	1b RESTRICTIVE MARKINGS
2a SECURITY CLASSIFICATION AUTHORITY N/A since Unclassified	3 DISTRIBUTION/AVAILABILITY OF REPORT Approved for public release; distribution is unlimited.
2b DECLASSIFICATION/DOWNGRADING SCHEDULE N/A since Unclassified	
4 PERFORMING ORGANIZATION REPORT NUMBER(S)	5 MONITORING ORGANIZATION REPORT NUMBER(S) POR-2210 (EX) (WT-2210)(EX)
6a NAME OF PERFORMING ORGANIZATION U.S. Army Electronics Research and Development Laboratory 6b OFFICE SYMBOL (If applicable)	7a NAME OF MONITORING ORGANIZATION Defense Atomic Support Agency
6c ADDRESS (City, State, and ZIP Code) Fort Monmouth, NJ	7b ADDRESS (City, State, and ZIP Code) Washington, DC
8a NAME OF FUNDING/SPONSORING ORGANIZATION 8b OFFICE SYMBOL (If applicable)	9 PROCUREMENT INSTRUMENT IDENTIFICATION NUMBER
8c ADDRESS (City, State, and ZIP Code)	10 SOURCE OF FUNDING NUMBERS PROGRAM ELEMENT NO / PROJECT NO. / TASK NO. / WORK UNIT ACCESSION NO.

11 TITLE (Include Security Classification) OPERATION SUN BEAM, SHOT SMALL BOY; Project Officer's Report—Project 2.2, Measurement of Fast-Neutron Dose Rate as a Function of Time, Extracted Version

12 PERSONAL AUTHOR(S)
Kronenberg, S., Markow, B., Balton, I. A.

13a TYPE OF REPORT	13b TIME COVERED FROM ____ TO ____	14 DATE OF REPORT (Year, Month, Day)	15 PAGE COUNT
		631011	80

16 SUPPLEMENTARY NOTATION This report has had sensitive military information removed in order to provide an unclassified version for unlimited distribution. The work was performed by the Defense Nuclear Agency in support of the DoD Nuclear Test Personnel Review Program.

17 COSATI CODES		
FIELD	GROUP	SUB-GROUP
18	3	
20	8	

18 SUBJECT TERMS (Continue on reverse if necessary and identify by block number)
SUN BEAM
SMALL BOY
Neutron Measurement
Gamma Radiation
Calibration

19 ABSTRACT (Continue on reverse if necessary and identify by block number)

The dose rates of fast neutrons as a function of time were obtained. In view of the fact that the measurement of the neutron spectrum as a function of time was only an attempt and was instrumented very marginally, the objective of the experiment was achieved. However, because of the paucity of data points, the information was marginal and was obtained only because of multiple duplication at each station. The detectors worked well in all cases where they were not damaged by rough handling. The biggest drawback in the experiment was difficulty with electronic equipment, in particular with the amplifiers that had to be designed and built in the laboratory within a very limited time.

The reliability of the recorded data was good, and it was concluded that effects other than radiation did not influence the sensor outputs.

20 DISTRIBUTION/AVAILABILITY OF ABSTRACT	21 ABSTRACT SECURITY CLASSIFICATION
☒ UNCLASSIFIED/UNLIMITED ☐ SAME AS RPT ☐ DTIC USERS	UNCLASSIFIED
22a NAME OF RESPONSIBLE INDIVIDUAL MARK D. FLOHR	22b TELEPHONE (Include Area Code) (202) 325-7559
	22c OFFICE SYMBOL DNA/ISCM

DD FORM 1473, 84 MAR — 83 APR edition may be used until exhausted. All other editions are obsolete.

SECURITY CLASSIFICATION OF THIS PAGE
UNCLASSIFIED

FOREWORD

Classified material has been removed in order to make the information available on an unclassified, open publication basis, to any interested parties. The effort to declassify this report has been accomplished specifically to support the Department of Defense Nuclear Test Personnel Review (NTPR) Program. The objective is to facilitate studies of the low levels of radiation received by some individuals during the atmospheric nuclear test program by making as much information as possible available to all interested parties.

The material which has been deleted is either currently classified as Restricted Data or Formerly Restricted Data under the provisions of the Atomic Energy Act of 1954 (as amended), or is National Security Information, or has been determined to be critical military information which could reveal system or equipment vulnerabilities and is, therefore, not appropriate for open publication.

The Defense Nuclear Agency (DNA) believes that though all classified material has been deleted, the report accurately portrays the contents of the original. DNA also believes that the deleted material is of little or no significance to studies into the amounts, or types, of radiation received by any individuals during the atmospheric nuclear test program.

OPERATION SUN BEAM

SHOT SMALL BOY

PROJECT OFFICERS REPORT — PROJECT 2.2

MEASUREMENT OF FAST-NEUTRON DOSE RATE AS A FUNCTION OF TIME

Stanley Kronenberg, Project Officer

Basil Markow, Deputy Project Officer
I. A. Balton

United States Army Electronics Research
and Development Laboratory
Fort Monmouth, New Jersey

ABSTRACT

Fast-neutron intensity as a function of time was measured at 625, 1600, and 4,000 feet from a surface burst, with the use of a newly developed neutron detector. Project personnel also attempted to measure the fast-neutron spectrum as a function of time at the 1600-foot station.

The fast-neutron intensity was measured with a gamma-compensated neutron-sensitive SEMIRAD (secondary-electron mixed-radiation dosimetry). Basically, the SEMIRAD is a vacuum diode. Gammas produce Compton electrons in the wall, which, upon leaving the wall, produce low-energy secondary electrons. These electrons are collected on the other electrode. To make the SEMIRAD neutron-sensitive, the emitting wall must be made of either hydrogen-rich material or fissionable material. The neutrons then produce either recoil protons or fission fragments, which on leaving the wall, produce low-energy secondary electrons that are collected. Since the neutron-sensitive SEMIRAD is also gamma-sensitive, a bucking arrangement must be used with a neutron-insensitive SEMIRAD to eliminate the gamma sensitivity. The signal from this detector was recorded on both oscilloscopes and magnetic tape.

Measurement of the neutron spectrum as a function of time involved the use of another novel detector. The version used here had five elements. The individual element consists of a radiator

(In this case a hydrogen-rich plastic), an absorber (five different thicknesses were used), and an ionized-particle detector. Protons produced in the radiator are attenuated by the different thicknesses of absorber, depending on the proton energy. The protons are then detected by a silicon-diode particle detector. The signal current can be related to the original neutron spectrum by solution of the equation obtainable from the theory of the device.

Fast-neutron-intensity data as a function of time were obtained at all three stations. The duration of the fast-neutron environment was much shorter than anticipated.

The neutron signals at the two closer stations showed a rapid rise and then decayed within approximately 150 μsec. The sharp rise was apparently determined by the arrival of the and the relatively slow decay by the scattered neutrons. The peak dose rates were at 625 feet and at 1600 feet. At the 4000 foot station, the 14-Mev neutrons arrived separated in time from the fission neutrons.

For measurement of the neutron spectrum as a function of time, the data recovery was not complete; thus, analysis was impossible.

PREFACE

The following USAELRDL personnel contributed to the design, performance, and data analysis of this experiment and to the preparation of the report: Michael Basso, Alice Bogart, James Brown, George Bryan, Vernon Bryan, Frances Calafato, Gilbert Cantor, Charles Coates, Joseph Crotchfelt, George Fegan, Eric Ellstrom, Mildred Forsythe, William Gallas, Charles Ganers, Joseph Giacalone, Caroline Grossman, Gerald Healey, Bud Housfield, Ockle Johnson, Frank Kowalczyk, Ross Larrick, John D. Lloyd, William Lonnie, James McMahon, Edward Mocney, Venice Morris, Kristian Nilson, Charles Olsen, Charles Pullen, Richard Rast, Lillian Sacher, Albert Schwartz, John Schwartz, Loretta Schaad, Linda Solcum, Robert Steinek, Lillian Steelman, and Harry Van Gorden.

CONTENTS

FIGURES

CHAPTER I

INTRODUCTION

1.1 OBJECTIVES

The primary objective of Project 2.2, Shot Small Boy, was to obtain measurements of fast-neutron intensity as a function of distance and time

Project 2.2 measurements were made to enable establishment of the influence of fast neutrons on the gamma-rate measurement as the result of direct influence of fast neutrons on the gamma sensors and in the case where the fast neutrons produce gammas in the vicinity of the gamma sensors (e.g., shields, ground, etc.). Measurements were to be made at distances of 625, 1,600, and 4,000 feet from ground zero and for the following times: 0 to 50 μsec; 0 to 1,000 μsec; and 0 to 10 seconds (Figure 1.1). To find the influence of fast neutrons on the gamma measurement, approximate knowledge was needed of the fast-neutron spectrum and of how this spectrum changes with time at the point of the measurement. This measurement was to be made at the 1,600-foot station for times from 0 to 10 msec.

The secondary objective was to measure the fast-neutron rate as a function of distance and time as outlined above,

Such data were of interest

in connection with many problems, such as transient radiation effects on electronic components. Knowledge of the neutron and the gamma environments would also be helpful in the construction of laboratory devices that simulate radiations delivered from atomic devices. These considerations also apply to the fast-neutron spectrum as a function of time.

1.2 BACKGROUND

Measurements of the gamma dose rate as a function of time were never made before for the times and distances outlined in Section 1.1. In the past, measurements covered the alpha rise of the radiation very close to the device and the gamma rate as a function of distance and time at about 2,000-foot distances for times later than 1 msec. The latter measurement, which was made on Operation Plumbbob (Reference 1), is described in Chapter 2.

1.3 THEORY

1.3.1 General. One reason advanced for the lack of gamma-rate information for times between 1 μsec and 1 msec is that within this time interval, fast neutrons from the fission reaction arrive at distances between several hundred and several thousand feet from ground zero and affect the ion-chamber as well as the phosphor-plus-light sensor instrumentation. At some distances and times, the fast-neutron rate may be much higher than the gamma rate, and thus the gamma data may be very doubtful. Therefore, for valid measurements, the fast-neutron rate and the fast-neutron spectrum as a function of time should be known at the point of the gamma measurement. Another reason offered is that the dose rate changes very rapidly during the critical time interval. Therefore, instrumentation with high time resolution is necessary, and this instrumentation should be designed so as not to saturate at very high radiation levels. Hydrogenous phosphors used to record fast-neutron dose rates give excellent results for a rising radiation intensity, but when the intensity reaches a peak and starts to decline, results obtained with a phosphor-light detector system are doubtful. Therefore, this type of detector was not used in Project 2.2.

1.3.2 SEMIRAD Triode. For the measurement of fast-neutron rates independently of gammas, in accordance with specifications of Project

2.2, the best possible system was the triode SEMIRAD (secondary-electron mixed-radiation dosimetry). This triode was essentially two diodes with one lead in common. (SEMIRAD can be built so as to be sensitive to neutrons only and highly insensitive to gammas.) This instrument was developed and tested successfully at the Sandia Pulsed Reactor Facility (SPRF), Albuquerque, New Mexico. However, it was never used before to measure neutrons from a nuclear device. In addition, instrumentation was under development to measure fast-neutron spectra as a function of time at high intensity and with high time resolution. As of this date, no previous attempt has been made to make this measurement. The U. S. Army Electronics Research and Development Laboratory (USAELRDL) intended to make only one rather rough measurement at the second station, splitting the energy spectrum into three parts, mainly to determine the operability of the system.

1.3.3 Shielding Against EM Effect. The EM effect from the device is very strong during the early times of the measurement; therefore, the influence of the EM effect on the measurement had to be eliminated. Every sensor above ground and every piece of recording equipment in the bunkers is a potential antenna that may pick up the EM signal. These instruments must therefore have tight electromagnetic shielding.

Theory indicates that a perfect electromagnetic shield can be obtained by surrounding the volume to be shielded in a vacuum-tight cover made of a perfect conductor. In the ideal case, the thickness of the shield is not important. In practice, however, the shielding

has to be thick and of a material with high conductivity and preferably high permeability. For the bunker construction, welded one-inch soft-steel plates were chosen for the inside of the concrete wall. The dome containing the radiation sensors was made of one-half-inch steel plates, and the pipe through which the coaxial cables were fed from the detectors to the recorders was made of heavy wall steel. Special precautions had to be taken to avoid EM leaking through the manhole and through the hard-wire connection that activated the cameras in the bunker from the control point. These precautions were accomplished by the use of metallic packing on the points where the manhole met its cover.

The cable that provided the signal to open the cameras was loaded with explosive and was destroyed immediately after transmission of the signal two seconds before detonation of the device. A spring-loaded plate then closed the small opening through which the cable entered the bunker. The equipment inside of the bunkers was powered from a battery bank whose output was converted to 110 volts ac by a motor-generator. Thus, the system was completely separated by steel from the outside world at time zero. A battery-driven timing switch opened all circuits at +2 minutes.

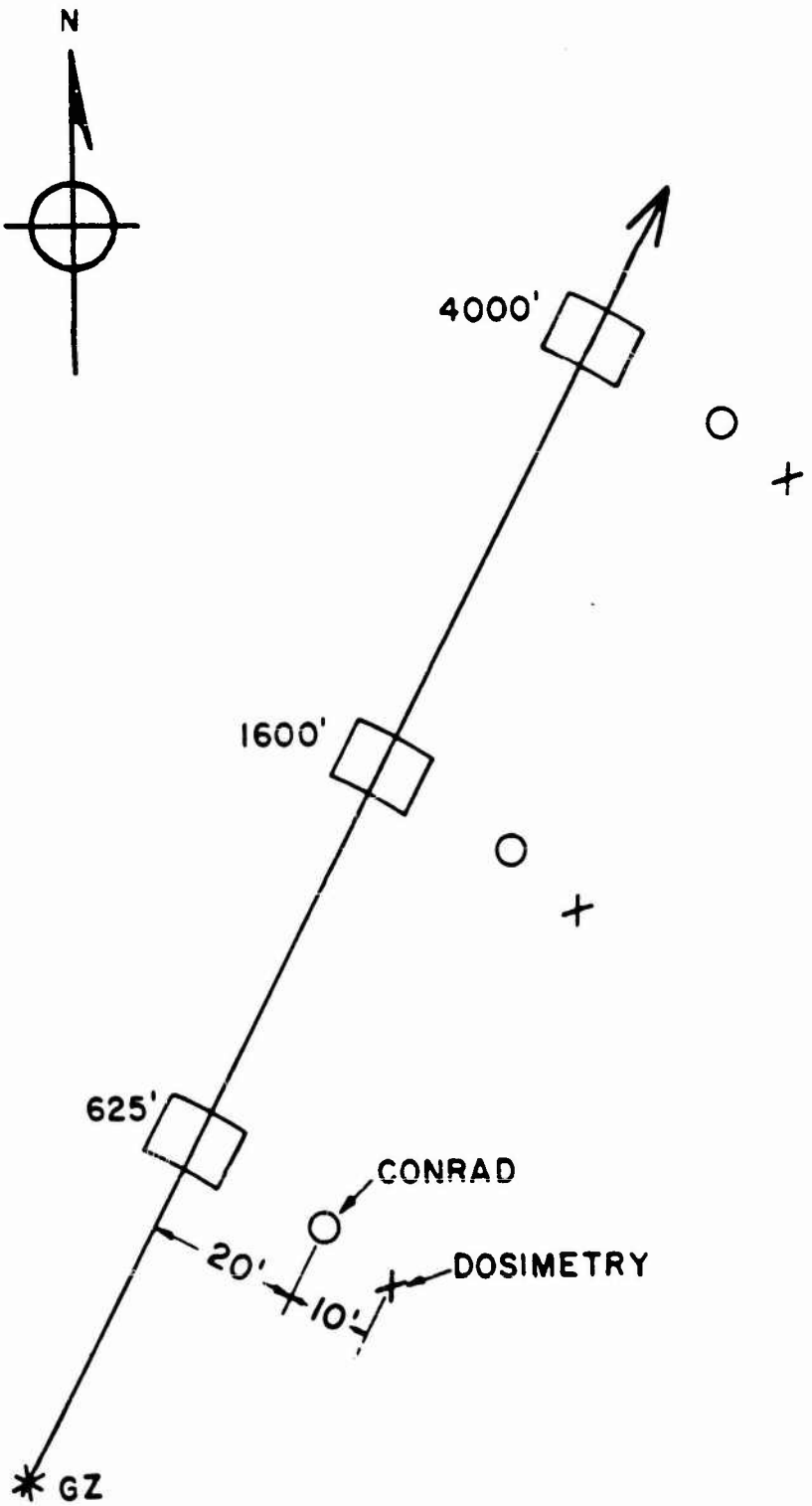

Figure 1.1 Station layout.

CHAPTER 2

PROCEDURE

2.1 OPERATIONS

2.1.1 Shot Participation. Project 2.2 participated only in Shot Small Boy. The device was to be symmetric with respect to the vertical axis, in order that the measurement on the ground would be as independent of direction as possible. The device was fired 10 feet above ground.

2.1.2 Test-Site Activities. All instrumentation was assembled and tested in the quonset area at the Nevada Test Site. Neutron detectors were calibrated at USAELRDL on the Van de Graff generator, tested on the SPRF, and again on a 100-curie Co^{60} source on site before shot time. Project oscilloscopes were serviced in the quonset area by a representative of the manufacturer.

The oscilloscopes were installed in the bunkers and the associated detector simulators positioned in their blast shields prior to the start of the preshot dry runs. Auxiliary equipment, as required, was used to check out systems and timing signals during the dry-run tests. Oscilloscope power supplies were checked during the dry runs.

The detector-tape system (CONRAD) was installed in each bunker, as well as in auxiliary locations outside each bunker. These systems were powered by nickel-cadmium batteries, which provided an

effective system life of five days in the field. The batteries were replaced on a four-day schedule during preshot dry-run periods. The auxiliary stations were entirely self-contained.

After completion of dry runs, final adjustments were made on oscilloscopes and cameras. Tape-recorder systems were loaded and secured. Power units were serviced and started as late as possible prior to evacuation. A last step was a camera record of each zero amplitude sweep on the oscilloscopes under latest-possible preshot conditions. A complete documentary photo of each equipment setting was required just prior to evacuation. After the inside of the bunker was secured, the access plug was inserted and sealed, using a heavy crane. This procedure also applied to Project 6.4.

All stations were activated by hard-wire timing signals furnished by Edgerton, Germeshausen, and Grier (EG&G). Timing-signal wires entering a bunker were destroyed just after the signal had activated the appropriate relay, in order to eliminate an effective antenna leading an EM pulse into the bunker. This requirement did not apply to the auxiliary stations.

Personnel-range gamma dosimetry was required inside the bunkers. Wide-range gamma dosimetry was required inside each blast shield, and a double set of gamma dosimetry (one for rapid recovery and one to await station recovery) was placed outside. Total-dose gamma dosimetry requirements were coordinated with the project responsible for gamma dosimetry: Nuclear Defense Laboratory (NDL), Army Chemical Center, Edgewood, Maryland. A complete set of neutron-foil measurements was required at or near the blast shield of each

bunker. In addition, gold and sulfur measurements were required inside and outside every blast shield and inside the connecting pipes. The neutron-measurement requirements were coordinated with responsible NDL personnel. These gamma-and-neutron dosimetry requirements also applied to Project 6.4

Re-entry was accomplished when Rad-Safe conditions permitted. When re-entry was accomplished, the stations were opened by a specially trained and prepared crew (a heavy crane was required for removal of access plugs). This crew photographed the instruments, removed plate holders from cameras, placed these holders in a lead box for fogging protection, and left the bunker expeditiously. Re-entry was a joint effort of Projects 2.2 and 6.4. Equipment and instruments of both projects were removed at a later date, after postshot calibrations were finished.

2.2 INSTRUMENTATION

2.2.1 Measurement of Fast-Neutron Fluxes in an Environment of Fast Neutrons and Gamma Rays. Considerable difficulties are inherent in attempts to measure the contribution of fast neutrons only, in a mixed fast-neutron-gamma environment. One can use either a fast-neutron-sensitive and gamma-insensitive device, or a device for measuring the gamma and the gamma-plus-neutron flux simultaneously, and subtract the readings.

Previously a system was used that consisted of two scintillation phosphors: one hydrogenous, and one hydrogen-free, each connected to a light detector. Such a device has two chief drawbacks: (1)

when the neutron flux is low compared to the gamma flux reasonably accurate neutron data is difficult to obtain; and (2) even a phosphor free of hydrogen responds to fast neutrons, due to recoil of atoms with $Z > 1$. By using two SEMIRADS, one of which is gamma-sensitive and the other both gamma-and-fast-neutron sensitive, and subtracting the readings, the second drawback can be eliminated to a high degree. Even if high-Z recoils are produced in the wall of the neutron-insensitive instrument, they will probably not enter the chamber and produce secondary electrons, because of the low-energy transfer between a fast neutron and an atom with $Z > 1$ and the resulting short range of the recoil. Use of two independent SEMIRAD does not help with the first drawback, and, thus, a more advanced system was designed.

Fast electrons (such as Compton electrons) and high-energy protons, when passing through an interface between a solid and vacuum, produce low-energy secondary electrons. A device based on this principle has been constructed (Figure 2.1). Compton, photo, or pair electrons, produced by incident gamma rays in the surroundings of the instrument or in the body of the instrument, produce secondary electrons from the thin metallic film with which the three plates are coated on their vacuum side. The structure of these plate surfaces facing the vacuum was made identical, and therefore the yield of the secondary electrons, which depends only on the structure of the emitter surface, was the same in all directions. The voltages applied to the plates were higher than the voltage corresponding to the energy of the secondary electrons. The polarity

of the voltages was such that the secondary-electron current reaching the central plate was the same as the outgoing current, and therefore the net external current produced by the gamma radiation measured between this plate and ground vanished. The primary electrons have a very high energy and cannot be influenced by the applied voltage. In the case of a monodirectional gamma flux, the central plate (hydrogenous material) provides an attenuation for the gammas and the net current does not quite vanish, but in a practical case this attenuation was made very small.

The two outer plates contain no hydrogen nor any material that would easily produce high-energy particles when reacting with neutrons. In the central plate, although it is made of a hydrogenous material on one side and a non-reacting material on the other, recoil protons are produced, some of which escape into the vacuum on the side where the evaporated metallic layer does not absorb them. When crossing the interface, these protons produce secondary electrons that can leave the plate on one side only and so produce an electric current proportional to the fast-neutron flux. This current is not compensated by another current and can be measured by an external meter or be displayed on an oscilloscope as a function of time. Thus, the fast-neutron flux can be determined independently of the simultaneously present gamma environment. Obviously, the fast neutrons also produce recoils with $Z > 1$ in the exterior plates. It can be shown, however, that because of their very short range, the probability that they will cross into the vacuum is very small. Their contribution to the measured current can be made negligible even for high-neutron-scattering cross sections.

The system works on secondary electrons alone and thus eliminates problems of saturation from ion recombination at high intensities. Its only limitation in dose-rate-output linearity comes from space charge (Langmuir saturation) at very-high-radiation dose rates. Its time response is very short (10^{-10} sec).

Figure 2.2 shows the actual construction of the instrument. The plates are circular and equal in area. The insulation between them is provided by alumina ceramic rings with Kovar flanges (metal-to-ceramic seal). The external plates are heliarc-welded to the flanges. The external plate facing away from the incoming radiation has two openings: one for a vac-ion pump used to monitor the vacuum and to improve it if necessary, and the other for the copper tubing for the tip-off. The outer Kovar plates are lined on the inside with aluminum plates. The aluminum was buffed to a high polish and then coated with a 0.1 mg/cm^2 layer of evaporated gold.

The central plate assembly is wedged between the two heliarc-welded flanges and consists of 1-mm-thick glossy Mylar on the side away from the incoming radiation and of 1-mm-thick aluminum on the side facing the incoming radiation. For best results, the Mylar should be as thick as the range of the highest energy proton expected in the environment. Again the sides facing the vacuum are coated with a 0.1 mg/cm^2 layer of gold that serves as the emitter for the secondary electrons and makes the Mylar surface conductive at the same time. The measured resistance of the gold layer was 0.1 ohm across the disc. The vacuum that could be obtained and permanently maintained in the system was approximately 10^{-6} mm Hg. This was made

possible only after elimination of the moisture from the Mylar by heating it in a vacuum at 150°C before the evaporation with gold. The assembly was then placed in a thin-wall brass can with three hermetically sealed coaxial-cable connectors, each of which was electrically connected to one of the three plates. The can was then filled with an insulating plastic potting compound to a level slightly above the top plate. The use of hermetically sealed connectors and the potting were most important here, because in that way the presence of air was avoided around the sensitive parts of the system. The presence of air would produce an unwanted ionization-chamber effect whose signal would be superimposed over the secondary-electron signal and give erroneous readings. Solid dielectric 70-ohm coaxial cable connected the can to a Keithley 610A electrometer for calibration. Two other cables supplied the necessary voltage to the outer plates (+ 300 volts, - 300 volts). After proper termination of the signal cable and connection with the readout scope located outside the radiation area, the instrument was ready to measure the neutron rate as a function of time.

To establish the X-ray sensitivity, or rather, insensitivity of the device, X-rays from a 250-kv machine and the output of the LINAC White Sands Missile Base, New Mexico, were used. The fast-neutron calibration was made using Be (D,n) neutrons from a 2-Mev Van de Graaff accelerator and the SPRF reactor, Sandia Corporation, Albuquerque, New Mexico. The signal current was measured with a Keithley 610A electrometer and, for high-intensity pulsed radiation, was recorded on oscilloscopes. At high dose rates (SPRF, LINAC) the

measured insensitivity for gamma radiation was less than 10^{-18} a/r/hr (amps/rad/hr) with +300 volts on the one and -300 volts on the other exterior plate. For equal polarity on the outside electrodes, the system became, in the absence of neutrons, a gamma-ray detector, and its sensitivity was 8.10^{-16} a/r/hr. The SPRF measurements yielded a sensitivity at 2.8×10^{-16} a/r/hr for fast neutrons (Watt spectrum). The calibrations at low-intensity steady-state radiation gave higher readings, because even with proper precaution, the cable effects contribute considerably to the readout at low intensities and thus falsify the calibration. At high intensities of radiation, the cable effects are saturated and therefore less pronounced. These effects were measured during the calibration at high intensity, and it was found that they are of the same order of magnitude as the gamma sensitivity of the SEMIRAD triode when it is compensated (approximately 10^{-18} a/r/hr).

Figure 2.3 shows a typical application of the instrument to measure the neutron output of a fast reactor (SPRF, Sandia Corporation, Albuquerque, New Mexico) as a function of time. The instrument followed the Godiva pulse very closely. The peak rate at the point of exposure was 1.5×10^{12} r/hr (fission neutrons).

2.2.2 Instrumentation for Measuring Fast-Neutron Spectra as a Function of Time. The theory of the fast-neutron spectroscope is described in the appendix of this report. In the design used on Shot Small Boy, solid-state detectors were used. Figure 2.4 is a diagram of the neutron spectroscope, and Figure A.2 is a photograph of this detector.

The instrumentation consisted of one unit placed at Station F, with five detector elements. Each detector element was made up of two parts, with separate detectors to cancel the effect of the gamma radiation by compensation. An hydrogenous emitter, polyethylene was used, and graphite was used for the nonhydrogenous part. The absorber was made of stacked aluminum foils. Table 2.1 lists the absorber thicknesses.

2.2.3 Sensitivity Calibration of the Fast-Neutron Spectrometer on the 2-Mev Van de Graaff Accelerator Using D(D,n) Neutrons. The crystal with the hydrogenous material and absorber (one aluminum foil) on top of it is placed in the neutron beam. Since the calibration requires a current measurement, a problem arises because the solid-state radiation detector operates with a reverse voltage bias. This results in a small dark current. This current is negligible during high-rate measurement, but during the low-rate calibration, it is several orders of magnitude higher than the signal current. Using the Wheatstone Bridge technique, shown in Figure 2.5, the dark current was cancelled out, and only the increase in conductivity from the neutrons was measured. The procedure was to balance the current through the electrometer to zero by the adjustment of either variable resistor A or B. Then the resistances R_1, R_2, and R_3 were measured, as was the voltage applied by the battery. This procedure was followed before and during neutron radiation. From the data obtained, R_x and the current flowing through that leg of the bridge circuit were computed.

$$R_x = \frac{R_1 R_2}{R_3}$$

$$i_{x_1} = \frac{V}{(R_x + R_1)}$$

By subtracting the current flowing through the spectrometer with and without neutron irradiation, the current produced by the recoil protons is obtained. Dividing this current by the dose rate, the sensitivity is obtained, which is dependent on the applied bias voltage. The results of the calibrations for a typical crystal are shown in Figure 2.6. For different crystals, the sensitivity as a function of voltage was almost the same. The sensitivity saturated at approximately 50 volts across the crystal, and, therefore, 60 volts was used during the field measurements.

2.2.4 Data Necessary for Decision on Recorder Sensitivity Settings

Considerable difficulty is involved in obtaining preliminary data on the fast neutron rates as a function of time to make possible the settings on sensitivity and sweep times. Attempts were made to estimate the rate as a function of time by using previous results on Godiva II (Figure 2.7). Through a rather far-fetched extrapolation, and with the well-justified presumption that the pulse length at the point of origin is small as compared with the pulse length at any one of the stations, the results shown in Figures 2.8 through 2.10 are obtained. These curves give an order of magnitude only, and as is evident from Project 2.2 results, this estimate exaggerated considerably the duration of the fast-neutron pulse. The estimate

is valid only for unboosted weapons. The oscilloscope settings at the stations used this estimate. Figures 2.11, 2.12, and 2.13 show the oscilloscope settings for the planned recordings.

2.2.5 CONRAD Instrumentation. To measure the gamma and neutron fluxes as a function of time at times later than 1 msec and up to 10 seconds, a modified CONRAD instrumentation was used. The sensors were ionization chambers. The readout system was self-contained, battery-powered, and used tape recorders. A CONRAD system was used on previous weapon tests and is described fully in Reference 1. Some previously unanswered questions include the reaction of CONRAD to the fast neutrons that are present together with the gamma rays and the contribution of gamma rays produced by the neutrons in the blast shield and instrument housing. To answer the above questions and to monitor independently the fast-neutron rate as a function of time, it was planned to use a modified CONRAD system together with the triode SEMIRAD as described earlier in this report. The signal from the neutron triode was amplified and recorded on a separate channel of the tape recorder. The pulse was recorded directly rather than using it to modulate the output frequency of the CONRAD system.

Two CONRAD systems were mounted on each station: one a self-contained system in a pit next to the bunker, and one with the detectors next to the other detectors in the instrument shield (which is an integral part of the bunker with the tape recorder in the bunker). Figures 2.11, 2.12, and 2.13 show the CONRAD and triode layout at the stations.

TABLE 2.1 DATA ON THE ELEMENTS USED IN THE FAST-NEUTRON SPECTROSCOPE

Element	Number of absorber foils	Absorber thickness	Proton energy cutoff
		mg/cm^2	Mev
1	1	4.3	1.18
2	3	12.9	2.24
3	9	38.8	4.27
4	500	$2.16 \cdot 10^3$	>15
5*	500	$2.16 \cdot 10^3$	>15

* No polyethlene used in this element

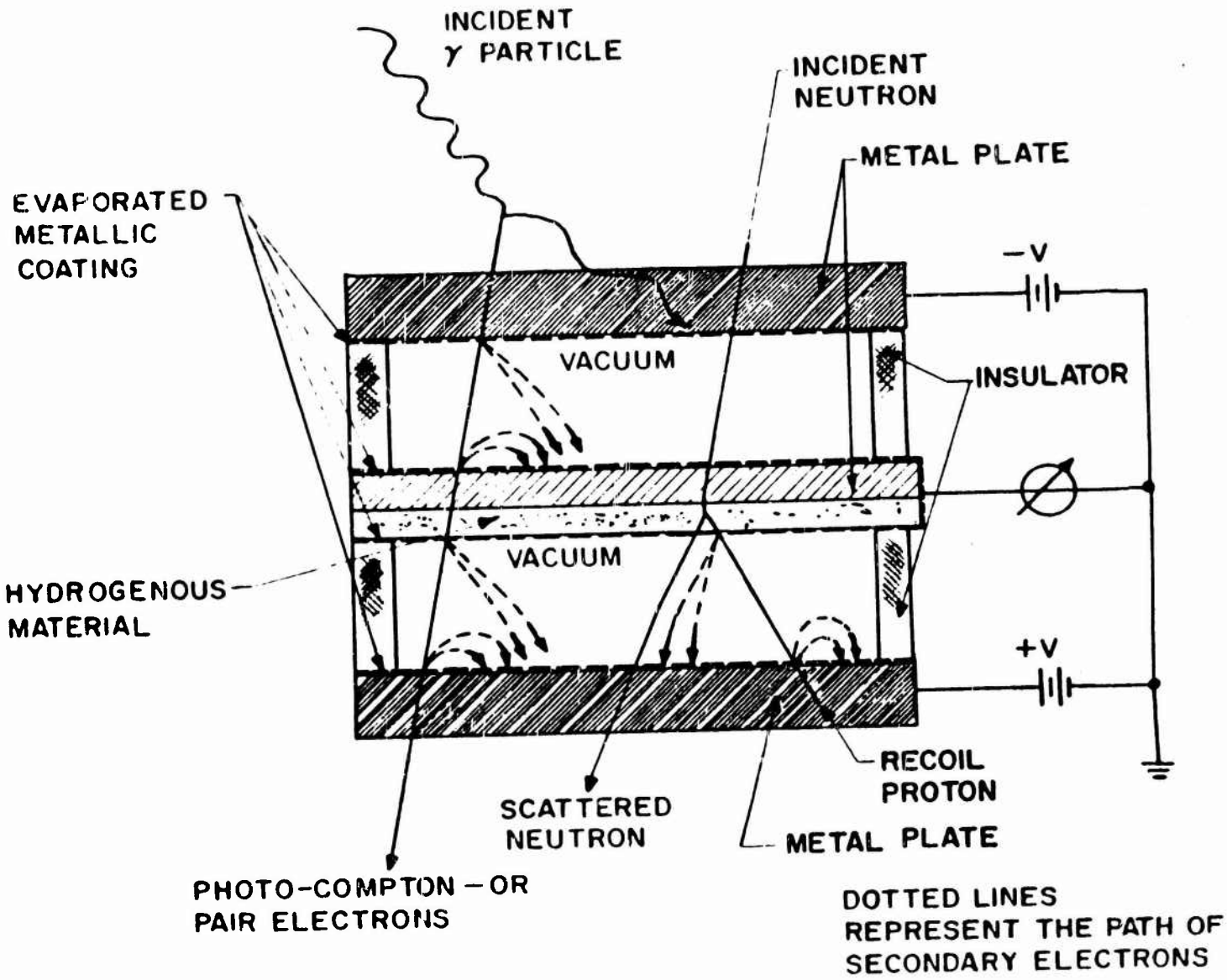

Figure 2.1 Principle of the fast-neutron SEMIRAD triode.

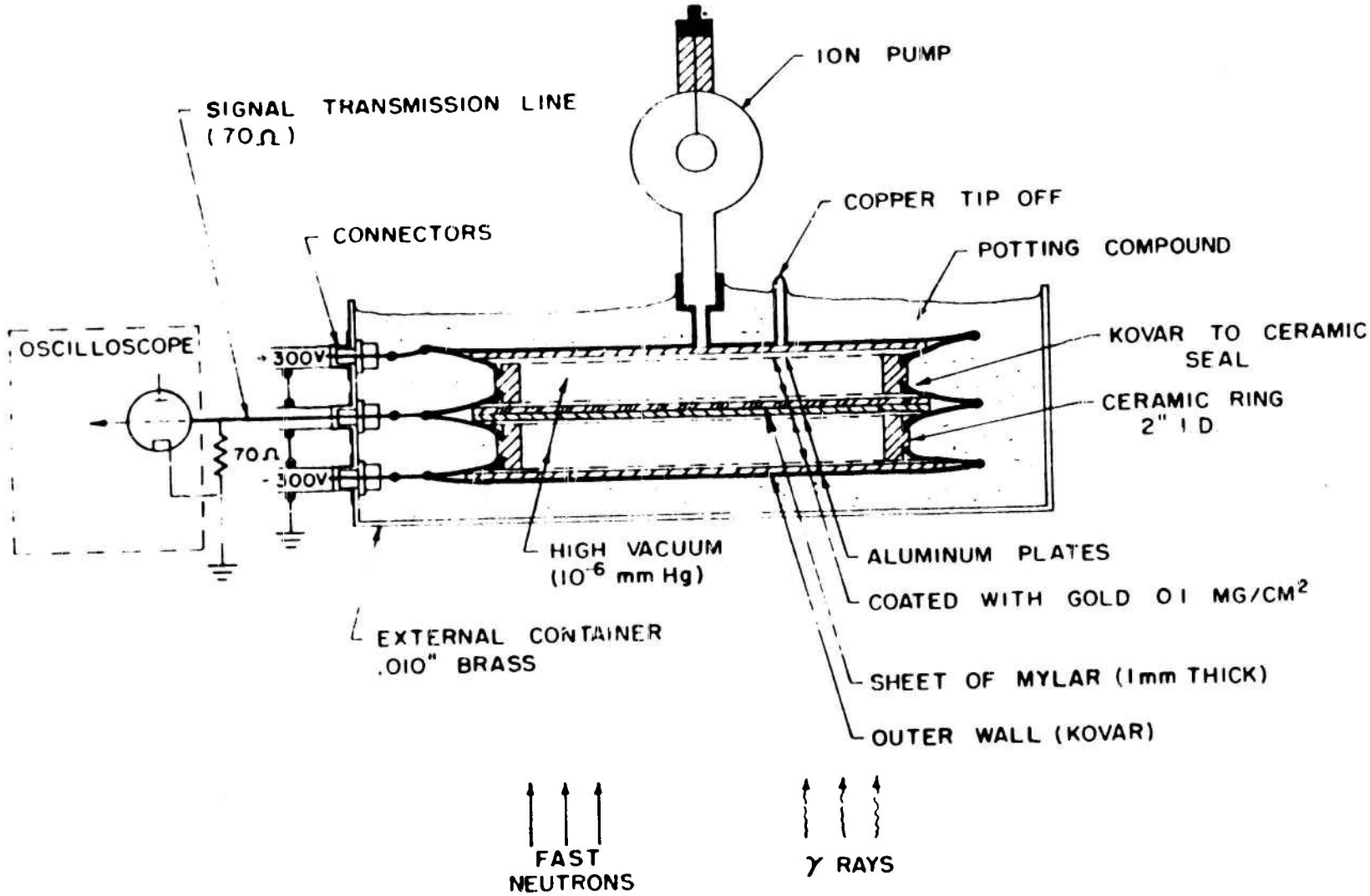

Figure 2.2 Construction of the fast-neutron triode.

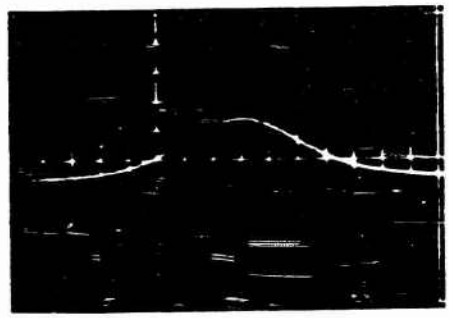

Figure 2.3 Measurement of the fast-neutron pulse from SPRF using the triode (sweep: 50 μsec/cm).

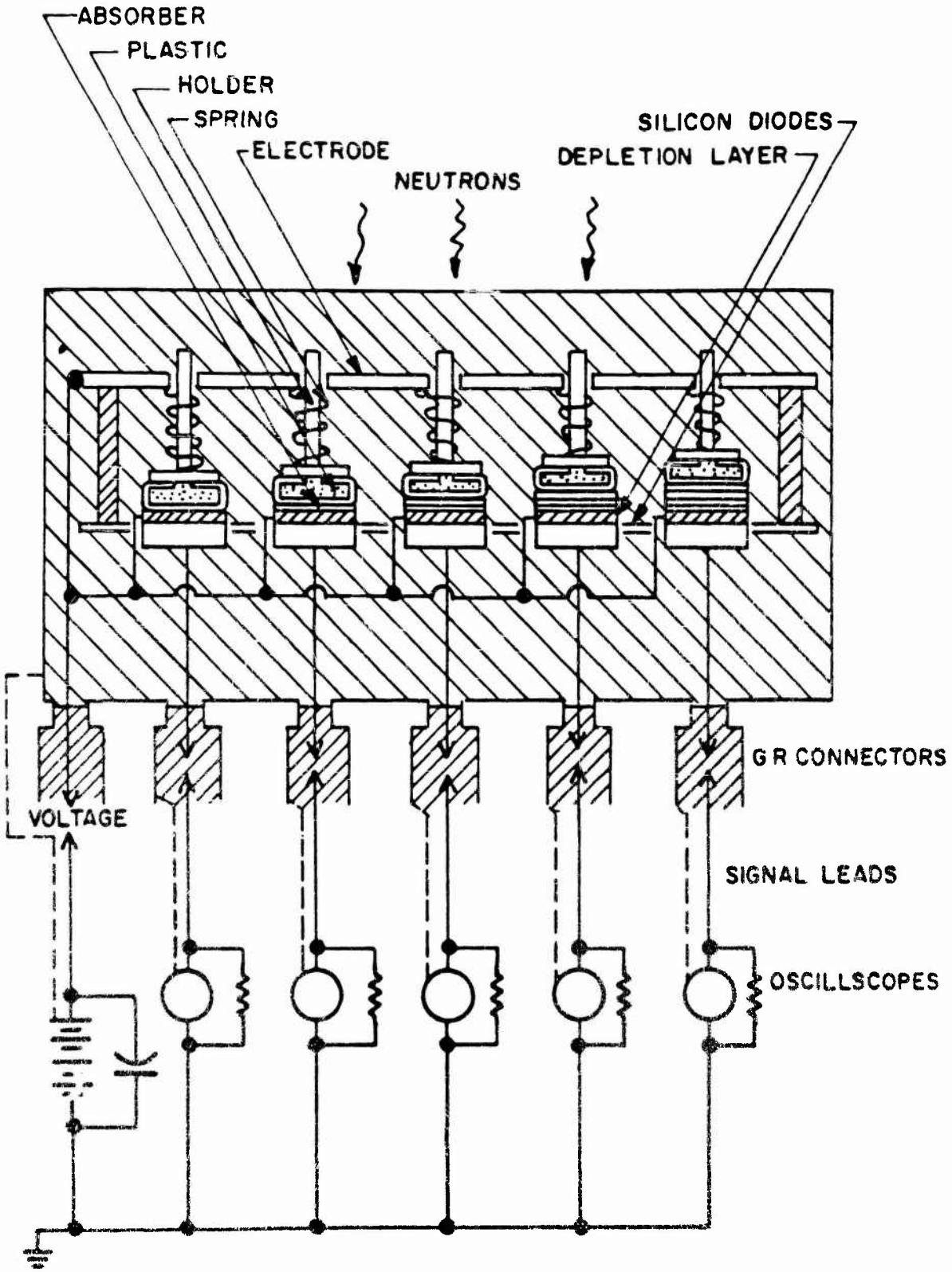

Figure 2.4 Fast-neutron spectroscopy system.

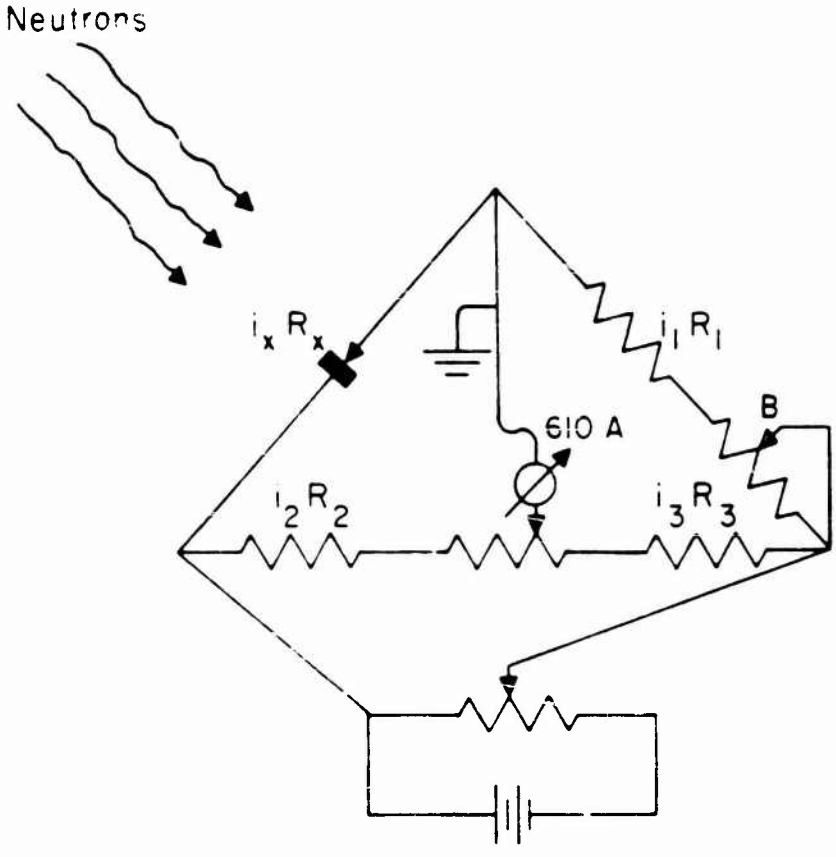

Figure 2.5 Instrument for calibration of the neutron spectroscopy system at low-dose rates.

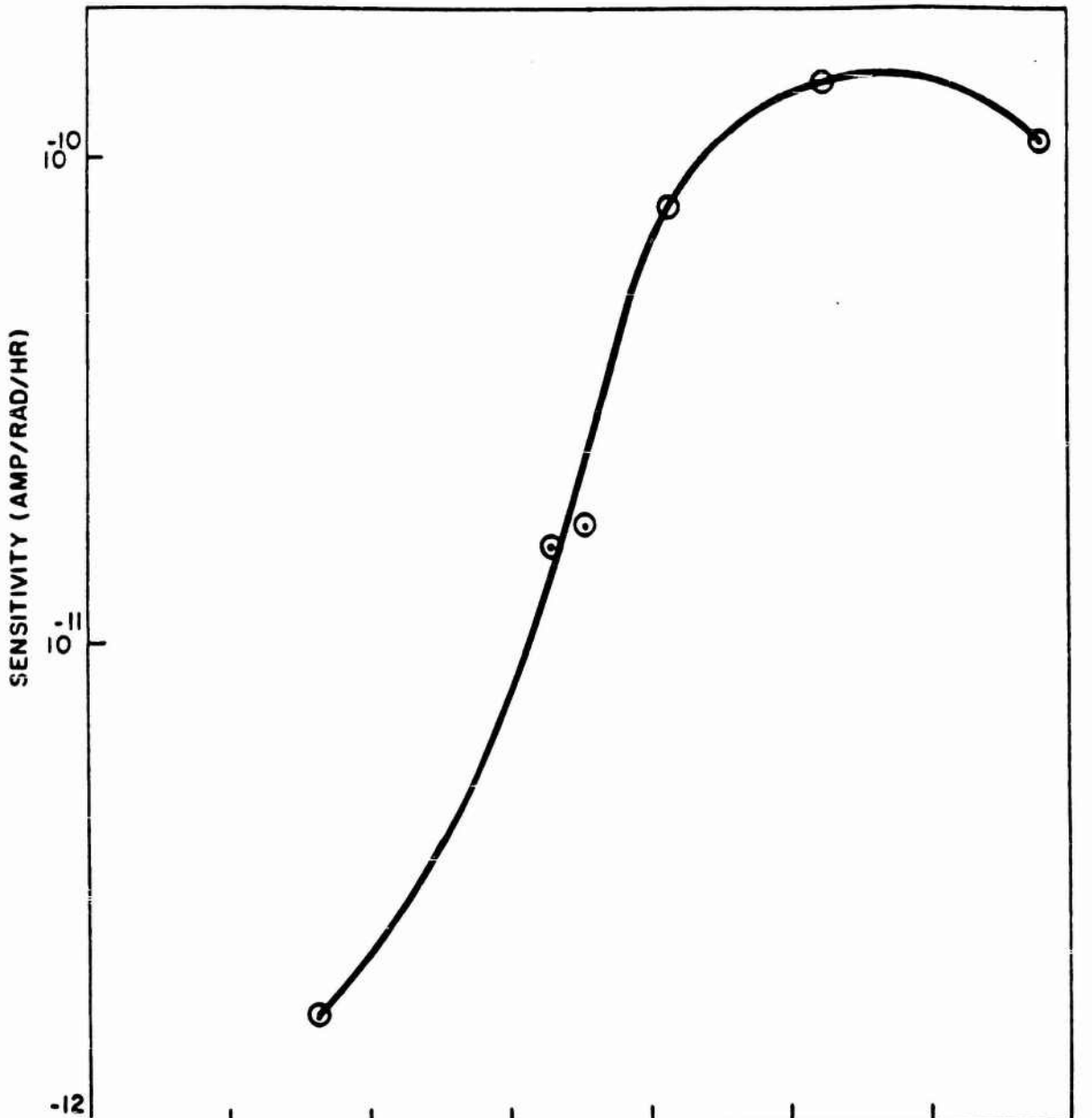

Figure 2.6 Calibration results of a typical silicon solid-state detector.

Pages 37 through 40
deleted.

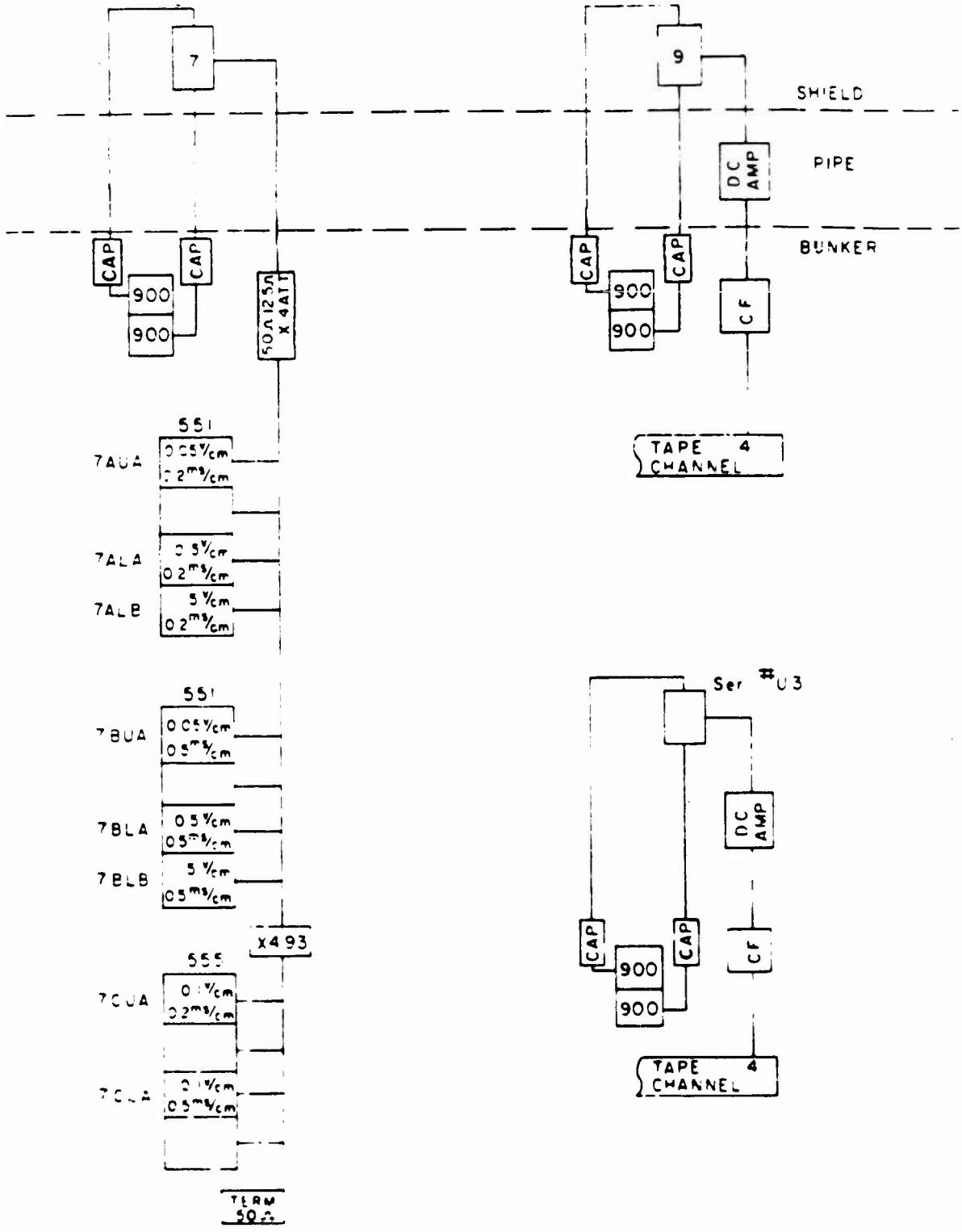

Figure 2.11 Sensitivity and time setting on recorders for Station E.

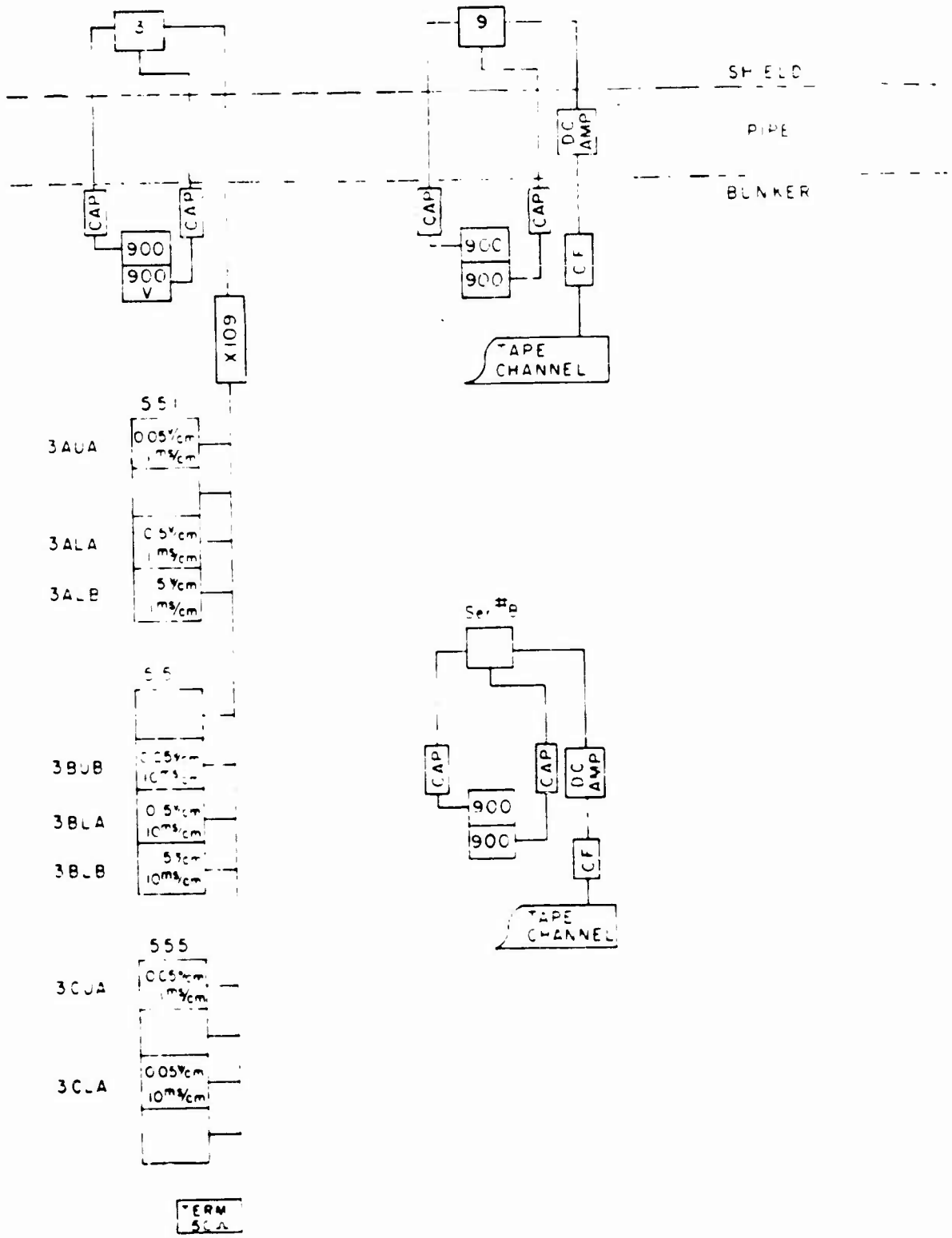

Figure 2.12 Sensitivity and time setting on recorders for Station F.

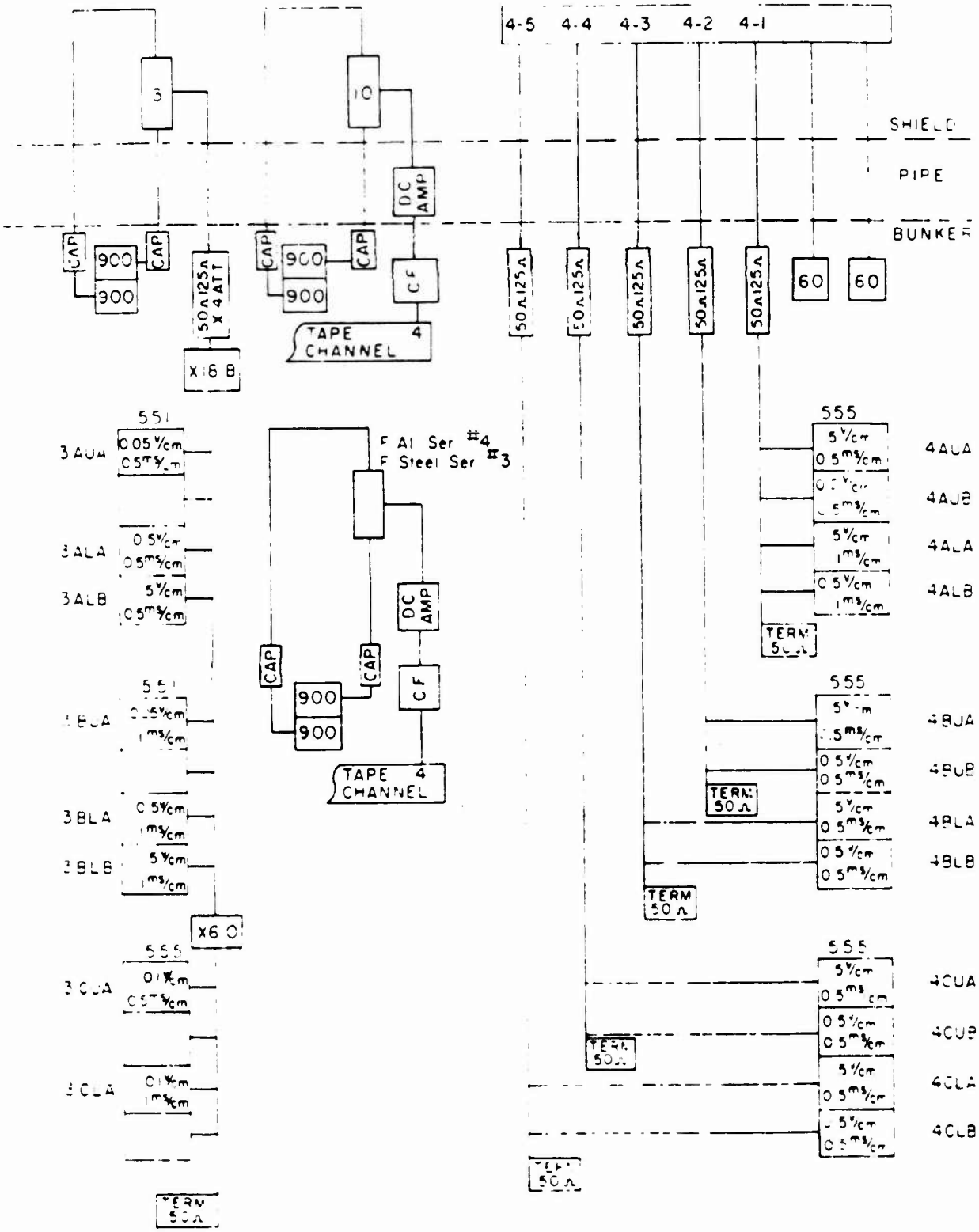

Figure 2.13 Sensitivity and time setting on recorders for Station G.

CHAPTER 3

PRESENTATION OF DATA

3.1 DETECTOR CALIBRATION

3.1.1 Total Dose

No neutron total-dose calibration was performed at the test site. The detectors (foils) were furnished by NDL, and all calibration and evaluation were done by Project 2.3 personnel.

3.1.2 Triode Calibration

Since no convenient pulsed neutron source was available, the neutron dose-rate detectors (triodes) were not calibrated at the test site. However, a continuous check of the vacuum within these detectors was made to insure that they would function properly at shot time. Whenever necessary the vac-ion pumps were used to bring the vacuum to an acceptable level (better than 10^{-4} mm Hg).

For the settings of recorder sensitivity, the pretest laboratory calibration of the triode was used. This sensitivity, 2.8×10^{-16} a/r/hr across 125 ohms resistance, amounted to 3.5×10^{-14} volts/r/hr. The calibration of the individual triodes varied from this value by a small amount. Every instrument was not calibrated individually because not enough time was available. Even if sufficient time had been available, such a calibration would not have been necessary, because the exact values of the calibration data have a tendency to shift with time and because in the final analysis, the sensitivity

computed in each case from the measured pulse shape and the measured total dose mainly was relied upon. The sensitivity obtained from the preshot calibration on SPRF was used only to determine oscilloscope settings.

3.1.3 The SPIDER Calibration. The SPIDER or neutron-spectrum detector was not calibrated at the test site. Therefore, the preshot laboratory calibration for the elements of this detector was used in this report. The sensitivity of the most sensitive element was 9.7×10^{-10} a/r/sec. The other elements in order of decreasing sensitivity were 7.75×10^{-10} a/r/sec and 5.8×10^{-10} a/r/sec.

3.1.4 Thermistor Temperature Detector Calibration. The temperature in the detector shield of the 4,000-foot station was remotely recorded on tape in the bunker by use of a thermistor and blocking oscillator from a standard radiosonde. Calibration of this temperature detector is given in Table 3.1.

3.2 AMPLIFIER CALIBRATION

3.2.1 Oscilloscope Amplifier Calibration. In addition to the built-in amplifiers, external oscilloscope amplifiers were built at USAELRDL. All amplifiers, both built-in and external, were calibrated before the event. The scopes on E yielded results from the triode and the scopes on F only for the SPIDER, and these calibrations are given in Tables 3.2 and 3.3.

3.2.2 Magnetic Tape Amplifier Calibration. The output of the triode was also recorded on magnetic tape. Since the signal was extremely weak, it was fed into a dc amplifier, then through a cathode follower, and then recorded on Channel 4 of the tape. No attempt was made to make this amplification linear over the entire frequency rang . It was considered better to determine the calibration over the entire range of recordable frequencies and use this information together with the Fourier Analysis of the pulse recorded on the tape to determine the shape of the true signal. It was later found that the rise times of most of the amplifiers were too long to record the dose rate correctly. The recording on G was calibrated, using a simulated input pulse similar to the result obtained at this station. Table 3.4 lists the amplification factors obtained with this method for the CONRAD stations.

3.3 SENSITIVITY

Figures 2.11 through 2.13 list the sensitivity setting and sweep speed for each signal trace on the oscilloscopes.

The traces are identified in the following manner: the first number indicates the number of the detector; the second place letter indicates the scope position in the series viewing the signal from the detector; the third position indicates which beam of a two-beam scope was used; and the fourth position indicates which chopped trace is indicated if the beam was chopped. For example, 4BUA is the trace

from detector #4; it is the second scope in the series as indicated by the letter B; it is the upper beam indicated by the letter U; and it is the upper trace of the chopped beam as indicated by the last letter A.

3.4 DATA

3.4.1 Total Dose. The dosimeters were made up into packages of the following types: Type 1 consisted of an NBS holder with 649-0, 508, 510, and 1290 emulsions; sulfur, gold, and cadium-shielded gold foils; glass rods with and without lithium shield, NBS film holder inside lithium shield (same emulsions as listed before), and chemical dosimeters. Type 2 consisted of an NBS film holder with 649-0, 508, 510, and 1290 emulsions; sulfur, gold, and gold in cadmium shield. Type 3 consisted of an NBS film holder with 649-0, 508, 510 and 1290 emulsions. Type 4 was a low-range film-dosimeter package.

A list of the total-dose dosimeters and their locations follows:

At the 625-foot station: A Type 1 dosimeter package was located both inside and outside the detector shield behind the collimator; inside the uncollimated instrument shield; in the drop station; inside the CONRAD shield; and fastened to the outside of the drop station. Two packages of quartz crystals and Battelle diodes were also fastened to the outside of the drop station.

At the 1,600-foot station: A Type 1 dosimeter package was located in the instrument shield, the aluminum CONRAD shield, and the steel CONRAD shield; inside the drop station; and taped to the outside of the drop station. In addition, quartz crystals and Battelle diodes were strapped to the outside of the drop station. A Type 3 dosimeter package was located at the mouth of the 8-inch cable pipe inside the bunker. A Type 4 dosimeter package was located at the center of the scope rack inside the bunker.

At the 4,000-foot station: A Type 1 dosimeter package was used inside the instrument shield; inside the CONRAD shield; inside the drop station; and taped to the outside of the drop station. A Type 3 dosimeter package was used at the mouth of the 8-inch cable pipe inside the bunker, and a Type 4 package was used at the center of the scope rack inside the bunker.

In addition to the above dosimetry, each station was to have threshhold type neutron detectors with a pull-out. Table 3.5 shows the total-dose results based on and including the data supplied by Project 2.1. The data recorded by USAELRDL is also included in this table. The total-dose measurements performed in places different from the location of the detectors did show in every case very low doses that could not possibly have affected the data. These recordings are not tabulated here.

3.4.2 Neutron-Dose Rate Data.

The recovered neutron dose-rate data recorded on magnetic tape (CONRAD) was returned to the laboratory for analysis. The tapes were photographed on 35-mm movie film for final analysis, and polaroid still photos were taken at a sweep speed of 20 μsec/cm to give an indication of the neutron dose rates versus time.

The oscilloscope traces were evaluated by use of a Richardson Model VF-55M projector. Data was obtained in digital form, and it could be then evaluated in the terms of radiation intensity as a function of time. The curves plotted in terms of arbitrary neutron dose-rate units as a function of time show the true shape of the fast-neutron pulse. To obtain the data in absolute units (reps/hr), the curves were calibrated by use of the values for the total neutron doses that were provided by Project 2.1 (Table 3.5.) The area under each curve, which can be obtained by graphic integration, is proportional to the total fast-neutron dose. One unit of the area represents a product of the time unit and the absolute dose-rate unit. Therefore, the peak dose rate can be obtained by means of the expression:

$$\text{Peak dose rate} = \frac{\text{Total dose X peak height}}{\text{Time unit(hours) X Area.}}$$

The SEMIRAD triode pulses that were recorded on magnetic tape (CONRAD) and later re-recorded in the form of pictures by the use of oscilloscopes are shown in Figures 3.1 through 3.4 for the CONRAD stations, F inside Bunker, F outside aluminum shielding, F

outside steel shielding, and G inside Bunker. In the CONRAD stations at E and at G outside the Bunker the equipment did not function, and no traces were recorded that can be related to nuclear radiation. The following oscilloscope recordings provided traces that can be related to nuclear radiation:

E 7CU, E 7CL, E 7AU, E 7ALA, and E 7ALB.

These recordings are shown in Figures 3.5 and 3.6. The sweep and amplitude settings are evident from Figure 2.11. The recordings of the spectroscopy system consist of the traces F4CUA, F4CUB, F4CLA, F4CLB, F4BLA, F4BLB, F4AUA, F4AUB, F4ALA, and F4ALB and are shown in Figures 3.7, 3.8, and 3.9. The sweep and amplitude settings of these traces are evident from Figure 2.12.

The following is a list of oscilloscope traces that did not yield any results. They include pictures where the scope did not sweep, where the film exposure was so low that even the strongest chemical intensification of the negative did not bring out the trace, and where the traces obtained had nothing whatsoever to do with radiation because of obvious electronic trouble:

G3CUA, G3CLA, G3BU, G3BLA, G3BLB, G3AU, G3ALA, G3ALB, G2AU, F3CU, F3CL, F3BU, F3BLA, F3BLB, F3AU, F3ALA, F3ALB, E7BU, E7BLA, and E7BLB.

TABLE 3.1 TEMPERATURE DETECTOR CALIBRATION AT THE SHIELD OF STATION G

°C	pulses/sec
25	54.3
30	62.5
35	72.9
40	88.4
45	102.0
50	117.9
55	133.3
60	142.8
65	154.0
70	180.0
75	186.6
80	200.0

TABLE 3.2 SCOPE SENSITIVITIES FOR TRIODE AT STATION E

(Based on $2.82 \cdot 10^{-16}$ a/r/hr triode sensitivity)

Scope	Sweep Speed	Dose-rate Sensitivity
	msec/cm	rad/hr/cm
E7AU	0.2	$8.10^2.10^{12}$
E7ALA	0.2	$8.10^2.10^{13}$
E7ALB	0.2	$8.10^2.10^{14}$
E7BU	0.5	$8.10^2.10^{12}$
E7BLA	0.5	$8.10^2.10^{13}$
E7BLB	0.5	$8.10^2.10^{14}$
E7CV	0.2	$8.10^2.10^{11}$
E7CL	0.5	$8.10^2.10^{11}$

TABLE 3.3 SCOPE SENSITIVITIES FOR SPIDER AT STATION F

Scope	Sweep Speed	Output Sensitivity
	msec/cm	v/cm
4AUA	0.5	0.562
4AUB	0.5	1.4
4ALA	1	0.562
4ALB	1	1.4
4BUA	0.5	0.562
4BUB	0.5	1.4
4BLA	0.5	0.562
4BLB	0.5	1.4
4CUA	0.5	0.562
4CUB	0.5	1.4
4CLA	0.5	0.562
4CLB	0.5	1.4

TABLE 3.4 SENSITIVITY VALUES FOR TRIODE RECORDINGS ON TAPE (OBTAINED FROM THE ELECTRONICS DATA)

(Based on $2.82 \cdot 10^{16}$ a/r/hr triode sensitivity)

Station	Sweep Speed	Recording Sensitivity
	μsec/cm	rep/hr/cm
F (bunker)	20	10^{13}
F (aluminum shield)	20	10^{13}
F (iron shield)	20	10^{13}
G (bunker)	20	$1.8 \cdot 10^{10}$

Pages 55 through 60
deleted.

CHAPTER 4

DISCUSSION

4.1 FAST-NEUTRON SPECTRUM AS A FUNCTION OF TIME

The oscilloscope pictures obtained in the experiment are shown in Figures 3.7, 3.8, and 3.9. Only traces for the detector with one and nine absorber layers were recorded. The detectors with three absorbers did not function. The element with 500 layers of absorber was expected to prevent all recoil protons from arriving at the detector to check on the performance of the system. As expected, no signal was obtained on this channel, which means that whatever was recorded on the channels that did show traces was a neutron signal. The last element that contained no hydrogenous material but carbon gave a signal, contrary to expectation. As was found later, some of the hydrogenous potting compound ran between the surface of the crystal and the absorber, giving rise to recoil protons. This trace is of no value to the experiment.

As explained in the Appendix, the spectrum as a function of time can be evaluated only if the width of energy intervals in which the spectrum is subdivided is sufficiently small so that the neutrons in each interval can be considered as monoenergetic. The fact that only two valid traces were obtained instead of three makes impossible the evaluation of spectrum as a function of time. With the present results the energy can be subdivided into only

two intervals 1.18 Mev through 4.27 Mev, and 4.27 Mev through 14 Mev, which are too wide for proper evaluation.

4.2 FAST-NEUTRON DOSE RATE AS A FUNCTION OF TIME

4.2.1 Station E (625 feet)

The SEMIRAD triode at this station gave results on all oscilloscope recordings (Figures 3.5 and 3.6.) The pulse is seen to rise very sharply, then decay very fast, and then more slowly. In all recordings the peak of the pulse is not well-defined; therefore, to determine the peak height of the pulse, the trace in Figure 3.5 was used. The undershoot of these traces comes from a poorly designed amplifier and is related to the pulse shape and height of the input. After the shot and using the original electronic equipment, pulses of the general shape of the pulse in Figure 3.5 were generated, and the peak height was varied until the undershoot of the output resembled closely that in Figure 3.5. The peak of the input pulse required to produce this same undershoot during this check must be the same as that in the original pulse. By means of this result and evaluation of the trace in Figure 3.6, the total-dose technique was used to arrive at the dose rate for fast neutrons as a function of time (Figure 4.1.)

4.2.2 Station F (1600 feet)

The fast-neutron pulse from the triode was recorded on all three CONRAD stations at Station F, but as mentioned earlier, the recording on the tape was not satisfactory because the time

resolution and amplification factor of the amplifiers were poor and also frequency- and amplitude-dependent. Figures 3.1, 3.2, and 3.3 show the records. The triode system recorded on the oscilloscopes did not function, and no data was obtained. Therefore, the only way to obtain the fast-neutron dose as a function of time at this station was to consider the recording of the fast-neutron spectroscope. The element of the spectroscope equipped with the thinnest absorber is compensated for gamma radiation, and its output, which was recorded correctly, gives the dose rate as a function of time as an approximately tissue-equivalent dose-rate meter for all neutrons with energy higher than 1.18 Mev (Figure 3.7.) This curve was evaluated by use of the total-dose method in terms of dose rate as a function of time and is shown in Figure 4.2. The intensity rises extremely fast when the 14-Mev neutrons arrive, and then decays rather uniformly to zero at Originally, we expected a double peak at this station: one from the 14-Mev neutrons and a second later peak from the fission neutrons. The measurement shows only one sharp peak, and this means that the valley between the two separated peaks was completely washed out by scattered neutrons. Also, as at Station E, the scattering of neutrons is responsible for the shape of the pulse to a much higher degree than the time of flight.

4.2.3 Station G (4000 feet)

At this station the traces from the triode in the bunker did not give any result, and only the CONRAD recording was satisfactory.

In general, the rise times of the pulses recorded on the tape were much shorter than the rise time on the scope pictures, because the amplifiers used at the CONRAD stations were poorly constructed and their output was slow and both frequency- and amplitude-dependent. After the evaluation of the data, an attempt was made to correlate the response of the amplifiers with the obtained pulses by use of the original equipment, with the result that only the CONRAD recording at Station G (Figure 3.4) seemed to approximate the true representation of the fast-neutron pulse. This was explained by the fact that the pulse width obtained was wider than the rise and decay times of the electronic system for the recorded pulse amplitude. This conclusion was checked later in the laboratory by insertion into the original electronic equipment simulated voltage pulses of varying width and height and recording the output. Starting with a pulse higher than the record at Station G, and with a width 1/2 of this recording, the pulse reproduction was fairly true for lower amplitudes and bigger widths.

An additional neutron result at Station G was obtained from the gamma measurement (Project 6.4). When the fast neutrons strike the instrument housing, part of their energy is converted into gamma radiation, which can be recorded. Figure 4.3 shows the oscilloscope

trace of this recording.

It is

interesting to notice that at the 4,000-foot distance, the 14-Mev neutrons and the Watt-spectrum neutrons are distinctly separated in time, while at the 625- and 1,500-foot distances, the separation between these peaks is completely washed out by scattering.

4.3 Additional Data

The temperature in the detector shield at the 4,000-foot station was measured and recorded on Channel 5 of the bunker tape recorder. It was constant at $19^{\circ}C \pm 1^{\circ}$.

Channel 6 of the tape recorders at all stations was a geophone placed on the floor of the bunkers.

Channel 7 on tapes recorded the output of a 10-kc timing oscillator. This recording worked only in the bunker stations, F and G.

Channel 8 was connected to the ac of the power lines through a filament transformer and in effect monitored the ac frequency and voltage in the bunkers during the shot.

The temperature in the bunkers was monitored during the event on a thermograph. Figures 4.6 through 4.8 are a record of this temperature.

Pages 67 through 71
deleted.

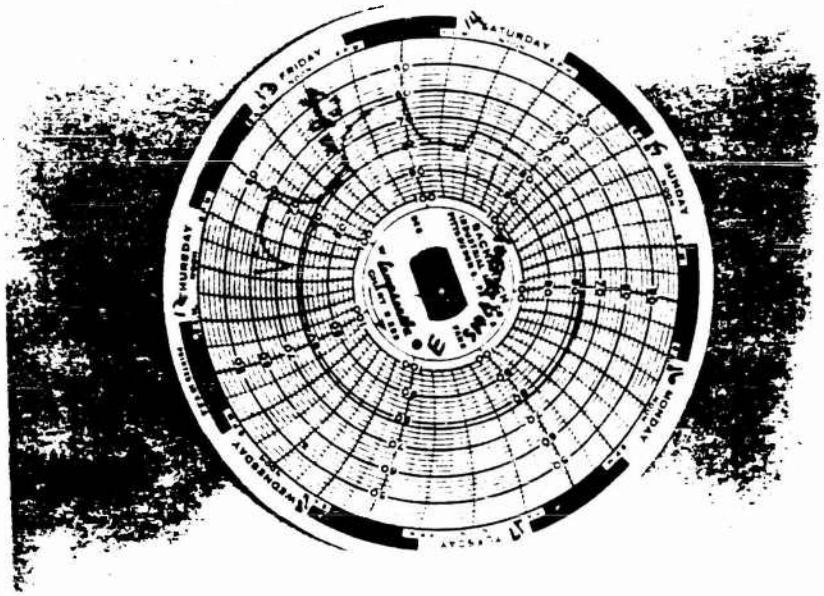

Figure 4.6 Thermograph recording at Station E bunker.

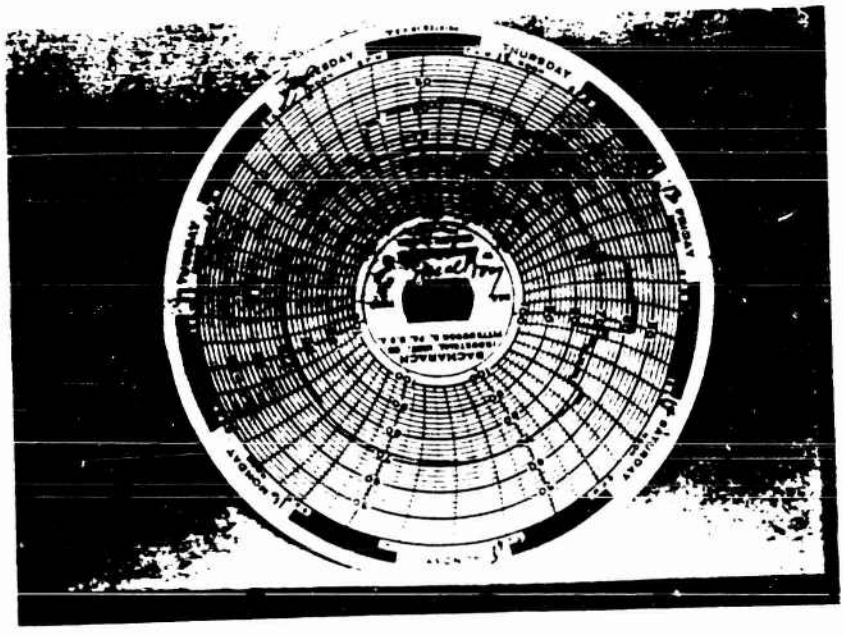

Figure 4.7 Thermograph recording at Station F bunker.

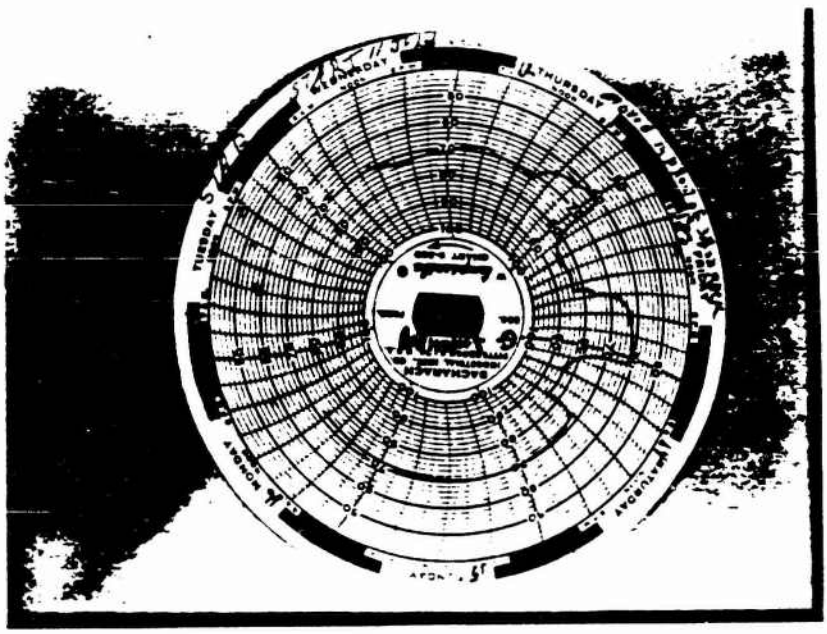

Figure 4.8 Thermograph recording at Station G bunker.

CHAPTER 5

CONCLUSIONS

The dose rates of fast neutrons as a function of time were obtained at all three desired locations. In view of the fact that the measurement of the neutron spectrum as a function of time was only an attempt and was instrumented very marginally, the objective of the experiment was achieved. However, because of the paucity of data points the information was marginal, and was obtained only because of multiple duplication at each station. The detectors worked well in all cases where they were not damaged by rough handling. The biggest drawback in the experiment was difficulty with electronic equipment, in particular with the amplifiers that had to be designed and built in the laboratory within a very limited time.

The reliability of the recorded data is good. Through analysis and postshot experiments, a decision was made as to which recordings were free of distortion due to poor electronics, and only acceptable recordings were used in the final data analysis. Project personnel also considered the possibility of distortion of the input signal by EM effect, radiation effects in cables, ionization, or other effects that are difficult to predict. Several approaches were taken to prevent these distortions or to correct them. The bunker stations were carefully shielded from EM and radiation. The hollow spaces between wires in the connectors, etc., were filled with

potting compound to prevent ionization, and the length of wire exposed to the direct nuclear radiation was made as short as possible. By placing two dummy instruments in the sensor heads at each bunker, a check was made as to whether the different effects influenced the measurements. The output of the dummies was recorded through the measurements. From 1 dummy at E, 1 at F, and 2 at G_r. no signal was recorded. One dummy at E gave a strong signal, but it was later found that the signal was due to ionization and the dummy was inoperative. Another dummy at F was interchanged erroneously with a gamma detector and therefore its readout system was set at self-triggering. It did not trigger at time zero but much later apparently when the shock wave arrived, which shows that around time zero no signal came from this dummy. It was concluded, therefore, that effects other than radiation did not influence the sensor outputs.

CHAPTER 6

RECOMMENDATIONS

Project 2.2 measurements were considered to be satisfactory, but a higher confidence level could be gained if a similar experiment were carried out in the future using the experience gained on Shot Small Boy. A future experiment should use much lighter but tightly EM-shielded confinement of the experimental arrangement than was the case in the Project 2.2 bunkers, improved and fast tape recorders with a time resolution of 10^{-6} seconds instead of slow-sweep oscilloscopes, and only a few fast scopes of the type 519 or memory cores for the earliest times. It is also imperative to use the highest quality electronic equipment available, or leave it out entirely. Future use of the fast-neutron SEMIRAD triode is recommended in all cases where the neutron intensity is very high, changes rapidly in time, and the neutrons arrive mixed with the gamma radiation.

The fast-neutron spectroscope is presently under construction in an advanced form, and after thorough laboratory use, may become available for field use.

APPENDIX

FAST-NEUTRON SPECTROSCOPE FOR MEASUREMENTS IN A HIGH-INTENSITY TIME-DEPENDENT NEUTRON ENVIRONMENT

A.1 INTRODUCTION

In modern research on pulsed reactors and other pulsed nuclear radiation sources, it is important to know the spectrum of fast neutrons in the environment of the source and how this spectrum varies with time during and after the pulse. Neutron spectroscopy as a function of time, using techniques of the single-particle energy analysis, cannot be applied because at high intensities it is not possible to resolve the single particles.

A device operating on the collective contribution of particles scattered by fast neutrons was designed and developed. It is designed to measure neutron spectra between the energies of several hundreds of kev and several tens of Mev when these neutrons are delivered at rates between $10^{2\epsilon}$ and $10^{1\epsilon}$ $n/cm^2/sec$. It can be modified for the fluxes between $10^{1\epsilon}$ and 10^{9} $n/cm^2/sec$ and for 10^{5} to 10^{4} $n/cm^2/sec$. The device may be constructed with a very high time resolution of about 10^{-9} seconds and is therefore capable of measuring a fast-neutron spectrum as a function of time when this spectrum is rapidly changing with time. The instrument can be made sensitive to fast neutrons and insensitive to gamma

radiation and beta rays, thus making it operative in a mixed radiation environment. This report describes the instrument for the intermediate intensity range ($10^{1\epsilon}$ to 10^{ϵ} n/cm^2/sec).

A.2 GENERAL DESCRIPTION OF THE DEVICE

The device consists of several similar elements with independent outputs placed close together in the neutron environment. The design of a single element of the spectroscope is shown in Figure A.1. It consists of a hydrogenous recoil proton emitter, which is thicker than the range of a proton with an energy corresponding to the highest neutron energy but much thinner than the mean free path of the neutrons being investigated in the environment. The emitter is surrounded by an absorber made of a homogenous material of constant thickness. The purpose of the absorber is to reduce, depending on its thickness, the energy and the number of the recoil protons escaping from the surface of the scatterer. The Z of the absorber material has to be much higher than 1 so that its recoils have a negligibly small chance of escaping through its surface, since heavy recoils have a short range as compared with protons and since the energy transfer between a neutron and a high-Z recoil is small. Pure aluminum can be considered a suitable absorber material. The absorber thickness is different for each of the elements

of the spectroscope, and the maximum absorber thickness is chosen so that none of the recoil protons can penetrate it. The absorber is surrounded by a detector. The same kind of detector is used for each one of the elements, and its design depends on the neutron intensity range in which the instrument is expected to function.

For intermediate neutron intensities (10^{16} to 10^{9} $n/cm^2/sec$), the detector should measure the total energy delivered to it by the recoil protons. Many different detector designs were applicable and the one used in Project 2.2 was based on solid-state detectors, where the output current was proportional to the total energy delivered to the detector as a function of time.

Knowledge of the output current enables one to obtain the spectrum of the neutrons incident on the detector as a function of time by use of the mathematical expressions derived in the following paragraphs. The neutron spectrum thus obtained will be in the form of a histogram with a constant or variable width of the intervals. The number of intervals of the histogram, which gives the resolution of the spectrum, will be equal to the number of elements used in the spectrometer.

A.3 MATHEMATICAL ANALYSIS

If a proton at rest is struck by a neutron of energy E_n, the proton after collision has the energy given by $E_n \cos^2 \varphi$ where φ is the angle between the original neutron velocity and the recoil proton velocity.

For the energy loss of these recoils in the traversed material, one can make the semi-empirical assumptions:

$$\frac{dE_p}{dX_H} = -K_H E_p^{Y_H} \qquad \text{(A.1a)}$$

$$\frac{dE_p}{dX_{AL}} = -K_{AL} E_p^{Y_{AL}} \qquad \text{(A.1b)}$$

Where: E_p = the proton energy

K_{AL}, Y_{AL} = material constants of the absorber

K_H, Y_H = material constants of the hydrogenous material.

X_{AL}, X_H = distance traveled in the absorber or in the hydrogenous material, respectively.

These relationships are correct for proton energies between 0.3 and several tens of Mev. When aluminum and polyethylene are considered as the absorber and scatterer material respectively, and the material thickness is expressed in a g/cm^2 rather than in cm, then $K_{AL} = K_H = K$ and $Y_{AL} = Y_H = Y$

Integrating Equation A.1a, a recoil proton with initial energy E_o after traveling a distance D in the scatterer is found to have the remaining energy E_1 given by:

$$\frac{E_o^{1-Y} - E_1^{1-Y}}{K(1-Y)} = D \qquad (A.2a)$$

In an analogous way, a proton that enters the absorber with energy E_1 and travels distance t, has the remaining energy given by:

$$\frac{E_1^{1-Y} - E^{1-Y}}{K(1-Y)} = t \qquad (A.2b)$$

Therefore, a proton that enters the detector after passing through the absorber and the scatterer has the energy E given by

$$\frac{E_o^{1-Y} - E^{1-Y}}{K(1-Y)} = D + t \qquad (A.3)$$

Protons of a single energy E_o are generated uniformly and isotropically throughout the irradiated slab. If N_o is the total proton activity, then $dN_o = ndX$, where n is the specific proton activity (number of protons generated per second in 1 g/cm^2 of the material). The number of protons in the solid angle defined in Figure A.1 by φ and $\varphi+d\varphi$ is

$$\frac{1}{2} ndX \sin \varphi \, d\varphi \qquad (A.4)$$

If a proton whose original energy was E_o is to emerge through D + t with an energy greater than E, then the maximum

value for D + t is given by Equation A.3. Consequently φ cannot exceed arc cos $\frac{X + T}{D + t}$, and the total number of protons that emerge from the absorber with energy greater than E and originate between X and X + dX is given by:

$$-\int_{0}^{\varphi_{max}} \frac{1}{2} n d(X + T) \sin \varphi d\varphi = -\frac{1}{2} n d(X + T) \left(1 - \frac{X + T}{D + t}\right) \quad (A.5)$$

with $\varphi_{max} = \arccos \frac{X + T}{D + t}$ (A.6)

The number of protons escaping from the whole radiator depth is then:

$$N(E_o) = -\int_{T}^{D+t} \frac{1}{2} n \left(1 - \frac{X + T}{D + t}\right) d(X + T)$$

$$= -\frac{1}{2} n \frac{1}{D + t} \left[(D + t) - T\right]^2 . \quad (A.7)$$

If there are protons with different original energies present, then there are $dN(E_o)$ protons in the energy interval dE_o and A.7 becomes:

$$dN(E_o) = -\frac{1}{2} dn \frac{1}{D+t} \left[(D + t) - T\right]^2 \quad (A.8)$$

If the protons are produced by monoenergetic neutrons of energy E_n, the recoil-proton spectrum at the point where the protons originate has a constant amplitude in $0 \leq E_o \leq E_n$, and is zero elsewhere. In this case, dn is proportional to the width of the corresponding energy interval ΔE_o, and can be expressed as:

$$dn = C dE_o = N_H A E_n^{-1} \sigma(E_n) h(E_n) dE_o \quad (A.9)$$

Where: N_H = the concentration of hydrogen atoms in the scatterer

A = the scatterer area,

The term $\sigma(Em)$, then is the $^{n-p}$ scattering cross section, and $h(E_n)$ is the flux of neutrons with energy E_n (monoenergetic).

To obtain the total number of recoil protons escaping to the detector, Equations A.9 and A.3 are substituted in A.8 and integrated over E_o. Since only the negative values of this function are physically meaningful, it is defined according to Expression A.8 only in the interval where its value is smaller than zero and has to be set equal to zero everywhere else. The limits of integration are therefore:

$$E_o = \left[TK(1-\gamma) + E^{1-\gamma}\right]^{1/1-\gamma} = \bar{E}_o(E) \qquad (A.10)$$

$$E_o = E_n$$

and

$$N = \frac{N_H A E_n^{-1} \sigma(E_n) h(E_n)}{4K(1-\gamma)} \int_{E_o=\bar{E}_o(E)}^{E_m} F(E_o E)\, dE_o \qquad (A.11)$$

$$\text{with} \quad F(E_o,E) = \frac{-\left[E_o^{1-\gamma} - E^{1-\gamma} - TK(1-\gamma)\right]^2}{E_o^{1-\gamma} - E^{1-\gamma}} \qquad (A.12)$$

Differentiation of A.11 with respect to E yields the spectrum of recoil protons originating in the scatterer and escaping through the absorber of thickness T:

$$\frac{dN}{dE} = \frac{C}{4K(1-\gamma)} \frac{\partial}{\partial E} \int_{E_o=\bar{E}(E)}^{E_n} F(E_o, E)\, dE_o \qquad (A.13)$$

In the case of A.11 and A.12 the following relations apply:

$$\frac{\partial}{\partial E} \int_{E_o=\bar{E}_o(E)}^{E_n} F(E_o, E)\, dE_o = \int_{E_o=\bar{E}_o(E)}^{E_n} \frac{\partial}{\partial E} F(E_o, E)\, dE_o \qquad (A.14)$$

$$\frac{\partial F}{\partial E}(E_o, E) = (1-\nu)E^{-\gamma}\left\{1 - \frac{T^2K^2(1-\nu)^2}{\left[E_o^{1-\gamma} - E^{1-\nu}\right]^2}\right\} \qquad (A.15)$$

Multiplying by E, considering A.14 and A.15., and integrating the resulting expression yields the total energy delivered by the recoil protons to the detector located at the absorber. The limits for this integration are the minimum and maximum proton energies that can contribute to the detector reading ($E = 0$ and $E = \left[E_n^{1-\gamma} - TK(1-\gamma)\right]^{1/1-\gamma}$; see Expression A.3)

$$E = \int_0^{\left[E_m^{1-\gamma} - TK(1-\gamma)\right]^{1/1-\gamma}} \frac{dN}{dE} E\, dE = \frac{C}{4K(1-\gamma)} \int_0^{\left[E_m^{1-\gamma} - TK(1-\gamma)\right]^{1/1-\gamma}} E\left[\int_{E_o=\bar{E}_o(E)}^{E_m} \frac{\partial F}{\partial E}(E_o, E)\, dE_o\right] dE \qquad (A.16)$$

Expression A.16 applies in the case of monoenergetic neutrons.

In the case of a neutron spectrum with the spectral distribution $h(E_n)$, the spectrum is subdivided into intervals of width ΔE_n, where E_n may be variable. Within each ΔE_n, all neutrons can be considered monoenergetic. There are $h(E_n)\Delta E_n$ neutrons in each interval, and, if k detector elements with different absorber thicknesses are available, Expression A.16 can be used for each of them. Therefore, for the delivery rate of the energy that can be observed with a detector belonging to an element whose absorber thickness is T_i, one obtains:

$$E(T_i) = \Delta E_1 h(E_1) A_{i1} + \dots \Delta E_K h(E_K) A_{iK} \qquad (A.17)$$

$i = 1, 2, 3 \dots$

Where: E_k = the highest neutron energy in the spectrum.

The constants A_{ij} are given by Expression A.13 and are:

$$A_{ij} = \frac{\sigma(E_j) A N_H}{4K(1-\gamma)E_j} \int_{E=0}^{[E_j^{1-\gamma} - T_i K(1-\gamma)]^{\frac{1}{1-\gamma}}} E \left[\int_{E_0=\bar{E}_0(E)}^{E_j} \frac{\partial F}{\partial E}(E_0, E)\, dE_0 \right] dE \qquad (A.18)$$

Where: E_j = the energy in the center of the interval ΔE_j.

Since k equations of the type A.17 are available, every $h(E_j)\Delta E_j$ can be computed. To evaluate the system in the case where it is intended to measure the number of protons escaping from the absorber per unit time as a function of time, expressions A.11 and A.12 are used. Integrating A.12 yields:

$$N = \frac{C}{4K(1-\gamma)} \int_{E=0}^{[E_m^{1-\gamma} - TK(1-\gamma)]^{\frac{1}{1-\gamma}}} \left[\int_{E_0 = \bar{E}_0(E)}^{E_m} \frac{\partial F}{\partial E}(E_0, E)\, dE_0 \right] dE \qquad \text{(A.19)}$$

where $\frac{\partial F}{\partial E}(E_0, E)$ is given by A.15.

From analogous considerations like those following A.12 we obtain

$$N(T_i) = \Delta E_1 h(E_1) B_{i1} + \cdots + \Delta E_K h(E_K) B_{iK}$$
$$i = 1, 2, \ldots K \qquad \text{(A.20)}$$

where the constants B_{ij} are

$$B_{ij} = \frac{\sigma(E_j) A N_H}{4K(1-\gamma) E_j} \int_{E=0}^{[E_j^{1-\gamma} - T_i K(1-\gamma)]^{1/1-\gamma}} \left[\int_{\bar{E}_0 = \bar{E}_0(E)}^{E_j} \frac{\partial F}{\partial E}(E_0, E)\, dE_0 \right] d(E \qquad \text{(A.21)}$$

$\mathcal{N}(T_i)$ is the total number of protons reaching the detector per unit of time, which can be measured experimentally. Again, the linear system for the $h(E_j)$ can be solved, which yields the neutron spectrum.

A.4 DISCUSSION

A.4.1 Evaluation of the neutron spectrum. In the previous section, it was shown that the fast-neutron intensity at the energy E_j within the energy interval ΔE_j can be obtained from the recorded data for one particular time (t) by evaluating the expression

$$h(E_\ell)\Delta E_\ell = \frac{\begin{vmatrix} a_{11} \cdots a_{1,\ell-1} & i_1 & a_{1,\ell+1} \cdots a_{1K} \\ \vdots & & \\ a_{K1} \cdots & i_K & \cdots a_{KK} \end{vmatrix}}{\begin{vmatrix} a_{11} \cdots a_{1K} \\ \vdots \\ a_{K1} \cdots a_{KK} \end{vmatrix}} \qquad \text{(A.22)}$$

regardless of whether the applied method is the measurement of the total number of recoil protons, or the total energy of recoil protons escaping through a set of absorbers with thickness $T_1 \ldots T_r$. Here a_{ij} are instrument constants that can be computed or determined by means of a laboratory experiment at very low neutron rates ℓ (single counts), using a monoenergetic neutron source. The $i_1(t) \ldots i_r(t)$ are the output currents or counting rates recorded through the detectors 1 through k at a particular instant of time. They represent either the proton current or the integral proton energy as a function of time. To obtain the neutron spectrum independently of a changing neutron flux one has to replace the currents $i_1 \ldots i_r$ by the numbers $\frac{i_2}{i_1} \ldots \frac{i_r}{i_1}$. Note that the value for $h(E_\ell)$ does not directly involve the spectral heights for energies higher or lower than E_ℓ, and therefore $h(E_\ell)$ can be evaluated independently for each energy interval and for each instant of

time. The evaluation of the linear system A.17 or A.20 becomes very simple if the determinant $|a_{ij}|$ is triangular or $a_{ij} = 0$ for $i > j$. The determinant can be obtained in this form by choosing the k absorber thicknesses T_i for each element so that each T_i forms a special relationship with the selected energy intervals ΔE_j at the energies E_j. By selecting T_i equal to the range of the proton of the energy E_i, only recoil protons that result from collisions with neutrons of an energy higher than E_i can possibly contribute to the detector current; and therefore $a_{ij} = 0$ for $i > j$. The range T_i of protons with the energy E_i can be obtained from Equation A.2b by setting $t = T_i, E = 0$ and $E_i = E_i$. Considering this choice for the absorber thicknesses, one obtains for the constants A_{ij} and B_{ij} in the linear systems A.17 and A.28

$$A_{ij} = \frac{\sigma(E_j)\, A\, N_H}{4\, K\, E_j} \int_{E=0}^{[E_j^{1-\gamma} - E_i^{1-\gamma}]^{\frac{1}{1-\gamma}}} E^{1-\gamma} \left[\int_{E_0=[E_i^{1-\gamma} + E^{1-\gamma}]^{\frac{1}{1-\gamma}}}^{E_j} \left\{ 1 - \frac{E_i^{1-\gamma}}{E_0^{1-\gamma} - E^{1-\gamma}} \right\} \sigma(E_0) \right] dE \qquad \text{A.23}$$

$$B_{ij} = \frac{\sigma(E_j)\, A\, N_H}{4 K E_j} \int_{E=0}^{[E_j^{1-\gamma} - E_i^{1-\gamma}]^{1/1-\gamma}} E^{-\gamma} \left[\int_{E_0=[E_i^{1-\gamma}+E^{1-\gamma}]^{1/1-\gamma}}^{E_j} \left\{ 1 - \frac{E_i^{1-\gamma}}{E_j^{1-\gamma} - E^{1-\gamma}} \right\} \phi(E_0) \right] dE \qquad \text{A.24}$$

Where: $a_{ij} = 0$ and $B_{ij} = 0$ for $i > j$.

These are the final expressions for the evaluation of the spectroscope system in the case where the total energy of the recoil protons is measured and for the case where the current or count rate of recoil protons is measured as a function of time, respectively.

A.4.2 Sensitivity of the device.

Expression 14 in Reference 2 gives the energy distribution of recoil protons escaping from the surface of a hydrogenous material irradiated with neutrons of the energy E_n. Multiplying this expression by the proton energy, integrating from zero to E_n with respect to E, substituting for the maximum range of the protons $\frac{E_n^{1-\gamma}}{K(1-\gamma)}$ protons (Reference 2), one obtains:

$$E = N_p E_n \frac{1-\gamma}{3-\gamma}$$

Where: N_p = the total number of escaping protons

E_n = the neutron energy

γ = the material constant in A.1a that has the typical value of -0.7.

In the case of 2-Mev incident neutrons, one obtains 57ev per incident n/cm^2/sec for the total energy delivered to the detector of an element with a very thin absorber. Considering the efficiency of the detector, which is $\sim$ 3 ev per free charge produced in a typical solid-state device, the sensitivity of the spectroscope element is obtained.

A.4.3 Operation of the system in a mixed environment of gammas and neutrons.

To measure the neutron spectrum in a mixed neutron-gamma environment, the spectroscope should be insensitive to gammas. In the version of the device discussed so far, the gamma rays produce fast electrons in every element of the device that may contribute to the output current. To avoid this one can apply a compensation method. Each element must be constructed as a double unit. One part of this unit is the regular element; the other is constructed with the same geometry but the hydrogenous material is replaced by a non-hydrogenous material, preferably carbon (pure graphite). The thickness of the carbon must be chosen so that its absorption

for gammas and its capability for fast-electron production is the same as for the hydrogenous layer. The outputs of both elements caused by gamma radiation are then almost equal, and if the outputs are connected so that the currents cancel each other, the device becomes gamma-insensitive to a high degree. The construction of the compensated device is shown in Figure A.2.

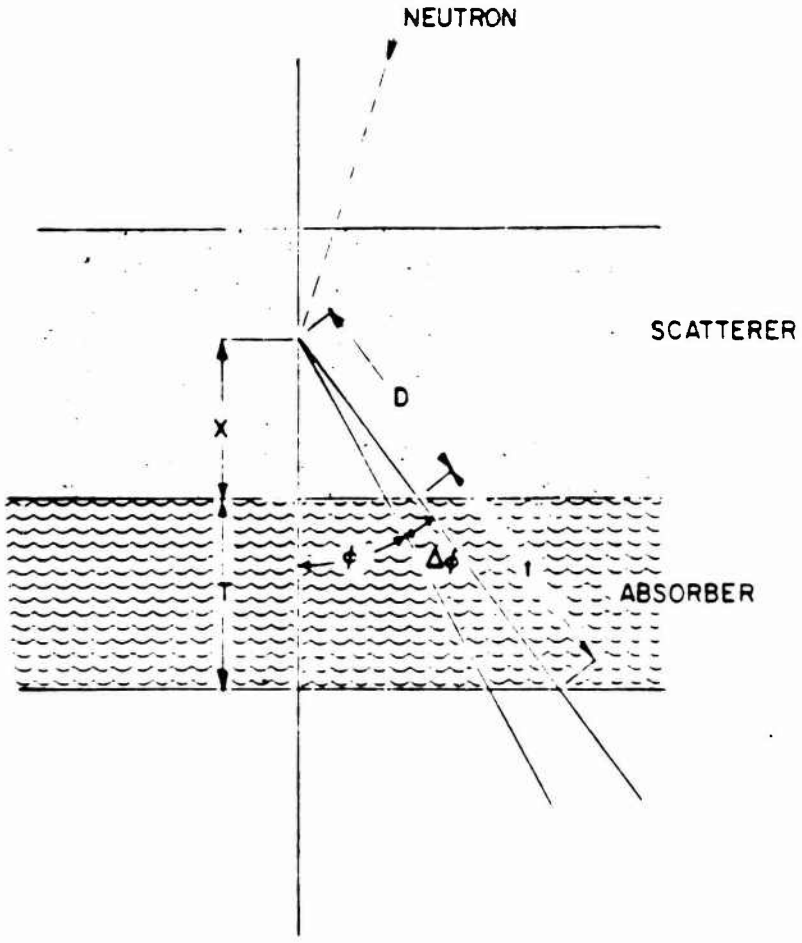

Figure A.1 Scatterer absorber system, showing the variables used in the computation.

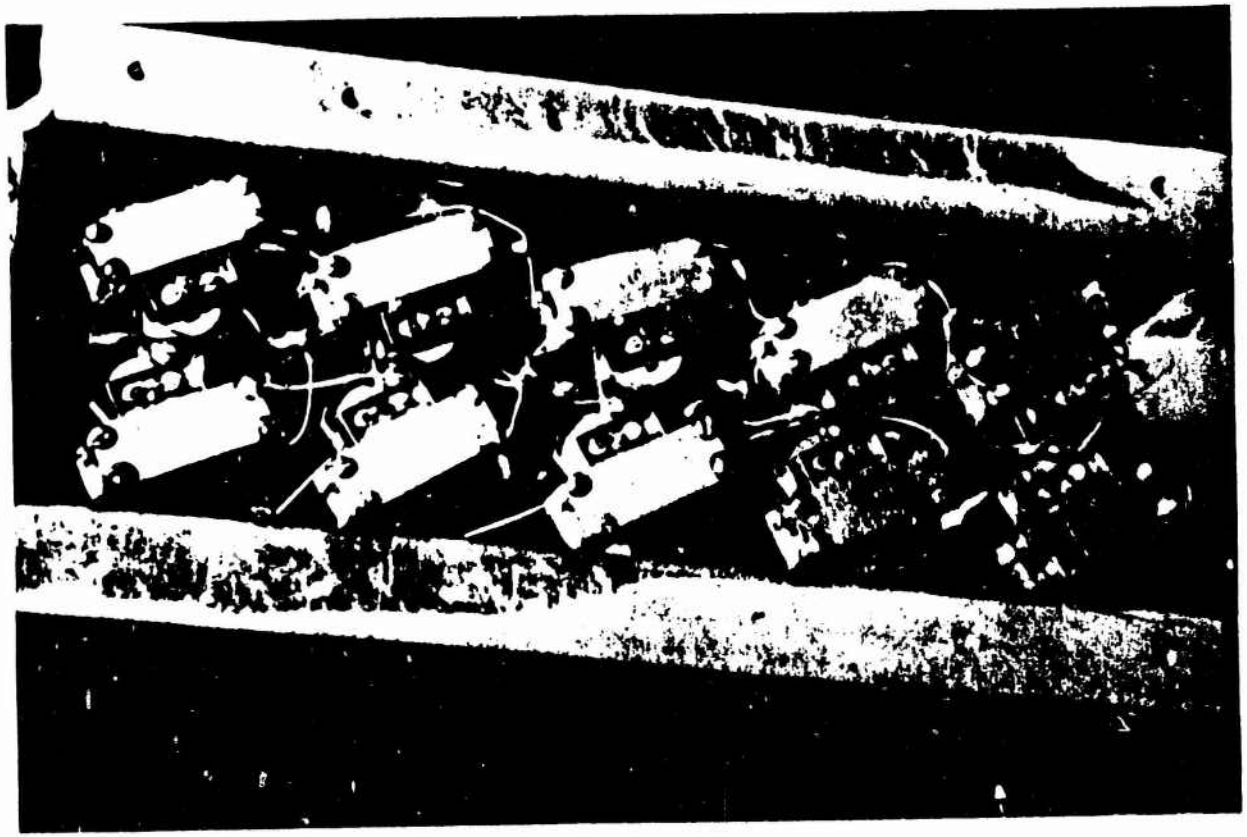

Figure A.2 Construction of a five-element gamma-compensated neutron spectroscope with silicon diodes used as recoil-proton energy detectors.

REFERENCES

1. G. Carp and others; "Initial-Gamma Radiation Intensity and Neutron-Induced Gamma Radiation of NTS Soil (U)"; Project 2.5, Operation Plumbbob, WT-1414, April 1961; U. S. Army Electronics Research and Development Laboratory, Fort Monmouth, New Jersey; Secret Restricted Data

2. S. Kronenberg and H. Murphy; Radiation Research 12, 728, 1960.

Page 97 deleted.